Model Predictive Control of Multilevel Power Electronic Converters

design, optimization and performance evaluation

Novak, Mateja

Publication date:
2019

Document Version
Publisher's PDF, also known as Version of record

MODEL PREDICTIVE CONTROL OF MULTILEVEL POWER ELECTRONIC CONVERTERS

DESIGN, OPTIMIZATION AND PERFORMANCE EVALUATION

BY
MATEJA NOVAK

DISSERTATION SUBMITTED 2019

AALBORG UNIVERSITY
DENMARK

Model predictive control of multilevel power electronic converters: Design, optimization and performance evaluation

Ph.D. Dissertation

Mateja Novak

Dissertation submitted November 7, 2019

Dissertation submitted: November 7, 2019

PhD supervisors: Assoc. Prof. Tomislav Dragicevic
Aalborg University

Prof. Frede Blaabjerg
Aalborg University

PhD committee: Associate Professor Amjad Anvari-Moghaddam (chair.)
Aalborg University

Professor Sergio Vazquez
University of Seville

Professor Alessandra Parisio
University of Manchester

PhD Series: Faculty of Engineering and Science, Aalborg University

Department: Department of Energy Technology

ISSN (online): 2446-1636
ISBN (online): 978-87-7210-535-2

Published by:
Aalborg University Press
Langagervej 2
DK – 9220 Aalborg Ø
Phone: +45 99407140
aauf@forlag.aau.dk
forlag.aau.dk

Printed in Denmark by Rosendahls, 2020

Abstract

Power electronics converters play an essential role in all stages of the energy conversion. Starting from the production units, until the final consumers are reached, power electronic converters are required to provide high efficiency energy conversion and quickly respond to changes in such stochastic environments. With the generation power installation size continuously increasing, more complex topologies have emerged to satisfy the high level requirements of energy conversion. A more complex topology will of course require a higher complexity of the control algorithm, that can incorporate all the non-linearities and the additional control objectives. Traditional cascaded linear controllers have dominated in the power electronics applications for many years. However, when designing and implementing these controllers, the non-linear power electronic converter systems have to be approximated by linear systems. This can lead to variation of performance. Moreover, multiple control objectives may slow down the response of the cascaded structures.

Finite set model predictive control (FS-MPC) algorithm comes from the family of non-linear algorithms and it is characterized by a straightforward design and a fast transient response. Multiple control objectives can simply be implemented in the cost function, which defines the desired behaviour of the converter. Therefore, one control loop can replace the nested control loops of the linear controller. Each objective in the cost function comes with a weighting factor, defining the importance of the objective.

Although many applications of the FS-MPC algorithm were proposed in power electronics, the algorithm has not yet fully reached the level of maturity observed for the linear controllers. For FS-MPC algorithm applications in power electronics, well defined design procedures and tools for assessing the performance and the stability are missing. The goal of this Ph.D. project is to propose new approaches and tools that can removed some of these limitations.

FS-MPC algorithm is an attractive alternative for multilevel converters, which due to higher number of devices and sources, require the implementation of additional control objectives. It is demonstrated that FS-MPC algorithm can not only be used to achieve a fast transient response and good reference tracking abilities, but is also able to extend the life-time of the three level neutral point clamped (NPC) converter. Uneven stress distribution, which is limiting the maximum output power of the converter, is a well-known problem of the neutral point clamped converter topology. The proposed FS-MPC algorithm can achieve a balanced stress distribution and reduce the junction temperatures of the most stressed devices. For the implementation, no additional measurements or device information are necessary. Moreover, FS-MPC algorithms can easily be adapted to optimize the operation of different hybrid configurations. In these configurations, the most stressed devices can be replaced with wide-bandgap devices, which can operate under higher voltages, temperatures and switching frequencies than silicon devices.

As mention before, each objective in the cost function is paired with a weighting factor. The tuning of these factors is not a trivial task and it can be time consuming if empirical methods are used. Therefore, an artificial intelligence aided design is proposed in this project for a fast optimization of the weighting factors with an analytical performance guarantee. Very good performance of high complexity optimizations in different converter applications confirmed the versatility of the proposed method.

If no simplifications or heuristic search algorithms are used, implementation of FS-MPC can become cumbersome on industrial microprocessor platforms for multi-step horizon algorithms and also for multilevel topologies with many switching combinations. Extending the prediction horizon can improve the control performance. When the prediction horizon is extended, the algorithm needs to find a sequence of switching actions that will minimize the cost function. Therefore, to reduce the computational burden of these applications, a solution based on artificial neural networks (ANN) is proposed. It was confirmed that ANN, a computationally light structure, can learn to imitate the FS-MPC algorithm with a very high accuracy. Even with an extension of the prediction horizon, the computational burden did not increase. This finding opens up opportunities for the implementation of not only FS-MPC algorithms but also to include an on-line tuning using new measurements to improve the controller performance.

Another contribution of this Ph.D. project is a performance verification tool for FS-MPC algorithm. FS-MPC algorithm is currently missing a universal approach to validate the performance in stochastic environments. The proposed approach uses statistical model checking (SMC), a powerful method for checking the performance of hybrid systems that feature both deterministic and stochastic behaviour. By running enough independent simulations, the SMC is able to predict the system behaviour. It offers the opportunity

to compare effects of different weighting factor combinations and parameter uncertainties on the control algorithm performance.

In conclusion, the contributions of this Ph.D. projects are aiming to remove the limitations of FS-MPC algorithm, show advantages of implementation on multilevel converters and propose tools that can validate and optimize its performance. Thus, it is anticipated that these findings can bring FS-MPC algorithm one step closer to more power electronics industrial implementations in the near future.

Dansk Resumé

Effektelektroniske omformere spiller en væsentlig rolle i alle faser af den elektriske energiomsætning. Startende fra el-produktionsenhederne (vedvarende energikilder) til de endelige el-forbrugere kræves effektelektroniske omformere for at levere en effektiv el-konvertering og hurtigt at kunne reagere på last ændringer. Da produktionen af el fra vedvarende energikilder konstant stiger (og størrelsen af enhederne stiger), er der kommet mere komplekse topologier (elektriske kredse) til at opfylde de høje krav til el- konverteringen. En mere kompleks topologi kræver oftere en højere kompleksitet af kontrolalgoritmen, der kan inkorporere alle ikke-lineariteter for at kunne opfylde nogle krav til en kontrol-performance. Traditionelle kaskade-koblede lineære kontrollere har domineret effektelektroniske apparater i mange år. Ved design og implementering af disse typer kontrol-enheder for de effektelektroniske omformere, der oftest er ikke-lineære, må der imidlertid tilnærmes til lineære systemer. Dette kan føre til variation i apparatets performance afhængig af arbejdspunkt. Samtidig kan flere kontrolmål nedsætte responsen fra de disse typer kontrol-strukturer, hvorfor andre kontrol strukturer er interessante at undersøge.

Finite-set model prediktiv kontrol (FS-MPC) kontrol algoritmen kommer fra familien af ikke-lineære kontrol strukturer, og den er kendetegnet ved et ligetil design og også havende en hurtig dynamik. Flere kontrol-mål kan simpelt implementeres ved hjælp af en speciel omkostningsfunktion i kontrol algoritmen, der definerer konverterens ønskede opførsel. En sådan kontrolstruktur kan erstatte de kaskade-baserede kontrolsløjfer. Hvert mål i omkostningsfunktionen har en vægtningsfaktor, der definerer målets betydning.

Selv om mange applikationer af FS-MPC-algoritmen er blevet foreslået i effektelektronisk omformere, har algoritmen endnu ikke fuldt ud opnået det modenhedsniveau, som allerede eksisterer for de lineære kontrollere. Til FS-MPC-algoritmeapplikationer i effektelektronik mangler veldefinerede designprocedurer og værktøjer til vurdering af ydelsen, samt til analyse af sta-

biliteten af hele systemet. Målet med dette ph.d. projektet er at foreslå nye metoder og værktøjer, der kan fjerne nogle af disse begrænsninger.

FS-MPC-algoritmen er eksempelvis et attraktivt alternativ for multi-level-omformere, som på grund af et større antal komponenter og spændingskilder kræver implementering af flere kontrolmål. Det demonstreres i afhandlingen, at FS-MPC-algoritmen både kan bruges til at opnå en hurtigere respons og har en god evne til at følge en reference, men er samtidig også i stand til at forlænge levetiden af en tre-niveau effektelektronisk omformer, som også kaldes en neutral-point clamped (NPC) konverter. En ujævn spændingsdeling imellem kondensatorerne, der ofte begrænser konverternes maksimale udgangseffekt, er et velkendt problem med NPC konverteren. Den foreslåede FS-MPC-algoritme kan opnå en afbalanceret spændingsfordeling og samtidig reducere temperaturerne for de mest stressede effektelektroniske komponenter. Til implementering af styre-metoden er der ikke behov for yderligere målinger og det er derfor en meget simpel metode, der er foreslået i afhandlingen. Derudover kan FS-MPC-algoritmen let tilpasses til at optimere driften af forskellige andre komponent-konfigurationer. I disse konfigurationer kan de mest stressede enheder erstattes med wide bandgap komponenter, som kan arbejde ved højere spændinger, temperaturer og switch frekvenser sammenlignet med silicium baserede komponenter.

Som nævnt tidligere er hvert mål i omkostningsfunktionen for FS-MPC forbundet med en vægtningsfaktor. Indstillingen af disse faktorer er ikke en triviel opgave, og det kan være tidskrævende, hvis der kun anvendes empiriske metoder. Derfor foreslås der i PhD afhandlingen at anvende en kunstig intelligensunderstøttet design-metode til en hurtig optimering af vægtningsfaktorerne med en analytisk garanteret performance. Der er opnået i afhandlingen en meget god ydelse af systemet via disse optimeringer, som har høj kompleksitet og det har bekræftet alsidigheden af den foreslåede metode.

Hvis der ikke anvendes nogen forenklinger eller heuristiske søgealgoritmer, kan implementeringen af FS-MPC blive besværlig på industrielle mikroprocessorplatforme, specielt for algoritmer der kigger længere ud i fremtiden end kun en samplingsperiode. Udvidelsen af forudsigelseshorisonten kan naturligvis umiddelbart forbedre kontrolydelsen, men når forudsigelseshorisonten udvides, skal algoritmen samtidig finde en sekvens af handlinger, der minimerer omkostningsfunktionen for FS-MPC. For at reducere beregningsbyrden for disse applikationer foreslås derfor en løsning baseret på neurale netværk (ANN). Det er blevet bekræftet i afhandlingen, at ANN er en beregningsmæssig let struktur at anvende og som kan lære at efterligne FS-MPC-algoritmen med en meget høj nøjagtighed. Selv ved en udvidelse af forudsigelseshorisonten (3-4 samples) steg beregningsbyrden ikke nævneværdig, når ANN blev anvendt. Denne erfaring åbner muligheden for implementering af ikke kun FS-MPC algoritmer, men også for at kunne inkludere

en online-optimering ved hjælp af nye målinger for at forbedre kontrollerens ydelse.

Et andet bidrag fra dette ph.d. projekt er udviklingen af et værktøj til eftervisning af ydelsen af FS-MPC algoritmer, hvilket hidtil har været meget vanskeligt. FS-MPC algoritmen mangler en universel tilgang til validering af ydeevnen i anvendelser med statistiske usikkerheder (stokastisk opførsel). Den foreslåede fremgangsmåde bruger en statistisk modelkontrol (SMC) algoritme, som er en kraftfuld metode til at kontrollere ydelsen af hybride systemer, der indeholder både deterministisk og stokastisk opførsel. Ved at køre en række uafhængige simuleringer er SMC i stand til at forudsige systemadfærden. Dette giver mulighed for at sammenligne effekten af forskellige kombinationer af vægtningsfaktorer og parameterusikkerheder i forbindelse med kontrolalgoritmen.

Afslutningsvis har bidragene fra dette ph.d. projekt kunnet fjerne nogle af begrænsningerne i FS-MPC-algoritmen, det har også vist fordele ved anvendelse af algoritmen på multi-level-omformere og samt foreslået værktøjer, der kan validere og optimere den foreslåede algoritmes ydeevne. Det forventes således, at disse bidrag kan bringe FS-MPC-algoritmen et skridt tættere på en mere industriel implementering i effektelektroniske systemer i den nærmeste fremtid.

Contents

Thesis Details

Thesis Title:	Model predictive control of multilevel power electronic converters: Design, optimization and performance evaluation
Ph.D. Student:	Mateja Novak
Supervisors:	Assoc. Prof. Tomislav Dragicevic, Aalborg University
	Prof. Frede Blaabjerg, Aalborg University

The main body of this thesis consists of the following papers:

Publications in Refereed Journals

J1. T. Dragicevic, **M. Novak**, "Weighting Factor Design in Model Predictive Control of Power Electronic Converters: An Artificial Neural Network Approach," *IEEE Trans. Ind. Electron.*, vol. 66, no. 11, pp. 8870–8880, Nov. 2019.

J2. **M. Novak**, H. Xie, T. Dragicevic, F. Wang, J. Rodriguez, and F. Blaabjerg, "Artificial Neural Network based weighting factor design for optimal control of the motor drives," *IEEE Trans. Ind. Electron.*, Status: Under Review.

J3. **M. Novak**, U. M. Nyman, T. Dragicevic, and F. Blaabjerg, "Analytical Design and Performance Validation of Finite Set MPC Regulated Power Converters," *IEEE Trans. Ind. Electron.*, vol. 66, no. 3, pp. 2004-2014, March. 2019.

J4. **M. Novak**, U. M. Nyman, T. Dragicevic, and F. Blaabjerg, "Application of Statistical Model Checking Methods to Finite Set Controlled Con-

verters," *IEEE Ind. Electron. Magazine*, vol. 13, no. 3, pp. 1–1, September 2019.

J5. **M. Novak**, T. Dragicevic, "Supervised Imitation Learning of Finite Set Model Predictive Control Systems for Power Electronics," *IEEE Trans. Ind. Electron.*, 2019, Status: Under Review.

Publications in Refereed Conferences

C1. **M. Novak**, T. Dragicevic and F. Blaabjerg, "Finite Set MPC Algorithm for Achieving Thermal Redistribution in a Neutral-Point-Clamped Converter," *Proc. of IECON*, Washington, DC, 2018, pp. 5290–5296.

C2. **M. Novak**, V. Ferreira, M. Andresen, T. Dragicevic, F. Blaabjerg, M. Liserre, "FS-MPC Algorithm for Optimized Operation of a Hybrid Active Neutral Point Clamped Converter," *Proc. of ECCE 2019*, Baltimore, MD, USA, 2019, pp 1–7.

C3. **M. Novak**, T. Dragicevic, and F. Blaabjerg, "Weighting factor design based on Artificial Neural Network for Finite Set MPC operated 3L-NPC converter," *Proc. of. APEC*, Anaheim, CA, USA, 2019, pp. 77–82.

C4. **M. Novak**, U. M. Nyman, T. Dragicevic, and F. Blaabjerg, "Statistical Performance Verification of FCS-MPC Applied to Three Level Neutral Point Clamped Converter," *Proc. of EPE 2018 - ECCE Europe*, Riga, Latvia, 2018, pp. 1–10.

This dissertation has been submitted for assessment in partial fulfilment of the Ph.D. degree. The thesis is a summary of the outcome from the Ph.D. project, which is documented based on the above publications. Parts of the results are used directly or indirectly in the extended summary of the thesis. The co-author statements have been made available to the assessment committee and are also available at the Faculty of Engineering and Science, Aalborg University.

Preface

The work presented in this dissertation was funded and carried out at the Department of Energy Technology, Aalborg University, Denmark. I would like to express my gratitude towards my supervisor Associate Professor Tomislav Dragicevic and my co-supervisor Professor Frede Blaabjerg for their guidance, support and patience during my Ph.D. study. Thank you for the encouragement and motivation that helped me complete this Ph.D. project. I would also like to thank Associate Professor Ulrik Nyman for introducing me to statistical model checking and UPPAAL software. Thank you for your guidance and help in developing the models.

I am grateful to Professor Marco Liserre for giving me an opportunity to join his research group at Chair of Power Electronics in Christian-Albrecht University of Kiel, and learn more about hardware and control design. I would also like to thank Dr. Markus Andresen and Victor Ferreira for interesting technical discussions and collaboration in building the experimental prototype. Thank you to the whole research group at Chair of Power Electronics for the nice hospitality during my stay.

I would like to also thank my colleagues at the Department of Energy Technology for their support and interesting discussions. Special thanks to Walter Neumayr for helping me in the laboratory.

Finally, I would like to thank my family and friends for supporting and encouraging me during my ups and downs. To my parents, who always found the right words of kindness and motivation when I was struggling and when my problems seemed bigger than they are.

Mateja Novak
Aalborg University, November 7, 2019

Part I

Report

Chapter 1

Introduction

"Strive for perfection in everything you do. Take the best that exists and make it better. When it does not exist, design it."

Sir Henry Royce

1.1 Background

Five important factors define the success factor of every emerging control method for power electronics converters: control concept simplicity, high-performance operation, robustness, proof of stability and versatility of the application [J3]. Due to these factors, for a very long period, the conventional cascaded linear control has dominated power electronic applications [1]. The design process of linear controllers is matured with well-defined guidelines for selecting the controller parameters, evaluating the performance and verifying the stability. However, power electronic converter systems are by nature non-linear systems, therefore to apply this conventional method, the system needs to be approximated with a linear system by using the pulse width modulation (PWM) techniques. Thus, some non-linear characteristics of the converter system can not be captured by a linear system model and this can as end-effect lead to limited performance. Also, to avoid overlapping in a cascaded structure system as shown in Fig. 1.1, the time constants of each outer loops have to be slower than the inner loop time constant. This of course will reduce the overall response speed of the controller.

A non-linear controller could therefore be a better option for power elec-

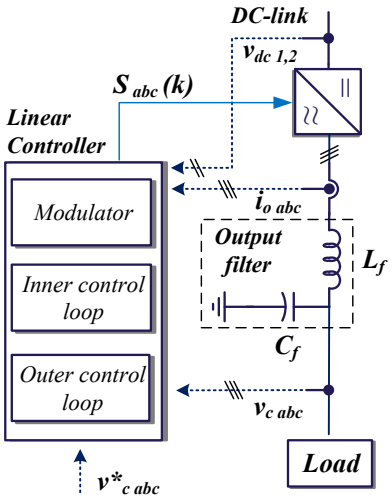

Fig. 1.1: Stand-alone converter system with conventional cascaded linear control.

tronics systems. The reason why non-linear controllers have been considered unpractical in the early stages of their development, is the disproportion in the available controller processing power and the computational burden of the algorithms. Nowadays, the processing power is increasing rapidly and advanced algorithms that were for long time living as an idea in the simulation software tools, are now ready for experimental validations and even industrial implementations [2, 3]. Another reason is lack of theoretical understanding.

One of the non-linear algorithms, that is receiving a lot of attention in power electronics now, is the finite set model predictive control (FS-MPC) algorithm [4]. The following three characteristics have contributed to the popularity of the algorithm. First, it is a simple control concept. The control objectives in FS-MPC control are defined through cost functions, which typically have the structure of square of Euclidean distances between the predictions of the controlled variables and the reference signals. Further, non-linearities like limitations of the converter current have a straightforward implementation. Not only reference tracking objectives can be included in the cost function, but also objectives like harmonics eliminations [5], common-mode voltage minimization [6], loss distribution[7], active thermal control [8], switching frequency minimization [9] have been applied. The high performance operation is a product of a single loop operation, without the cascade structure the response to disturbances is much faster [10]. Thus the control scheme from Fig. 1.1 is converted to the scheme shown in Fig. 1.2. Third, applications of the MPC have spread to almost all power electronic converter topologies

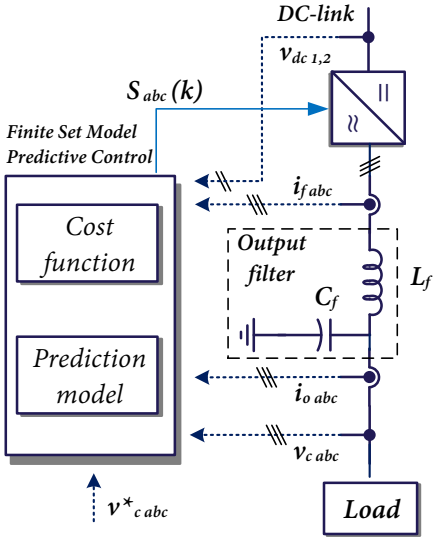

Fig. 1.2: Stand-alone FS-MPC controlled converter system.

[11], starting from the simple DC-DC boost topologies [12], two-level VSC converters popular for renewable energy applications [13] and drives [14, 15], multilevel converters [16, 17] and multi-cell converters [18].

Yet in many industrial applications linear control methods are still dominant while the FS-MPC is viewed as a research topic only. Nonetheless, there are three applications where model predictive algorithms can yield superior performance compared to the conventional linear control methods:

- Applications with many control variables. [19]
- Applications where the time constants are too close to each other.
- Applications with significant and dynamic cross coupling of the control variables. [10]

To come to the stage of industrial implementation in power electronics converters, versatile tools for optimizing the control algorithm design, performance and stability need to be developed for the FS-MPC algorithms [11, 20–22] .

1.1.1 FS-MPC algorithm for control of the NPC converters

With the power installation size continuously increasing, an efficient solution was needed to cover the wide voltage range of the power electronic converter

applications. Thus in 1981 [23] the first multilevel topologies were introduced to improve the efficiency of the variable speed drives. Although the initial applications were in medium and high voltage range [24], multilevel topologies have also been spread to the low voltage applications due to the lower total harmonic distortion (THD) of the output voltage, lower switching losses and converter filter size compared to the standard 2-level voltage source converters (VSC). Especially for interconnection of renewable energy sources, they have become an attractive alternative due to the before mentioned benefits [25, 26].

One of the multilevel topologies that very quickly spread to various applications is neutral point clamped (NPC) topology [27]. The configuration of one phase module is shown in Fig. 1.3. However, it was soon noticed that in some operating conditions of the converter, the uneven stress distribution was limiting the maximum output power and the switching frequency. Especially under nominal operating conditions or low voltage ride through scenarios, the design margins have to be adapted to the most stressed devices [28]. In 2001 a new topology was derived from the NPC topology by replacing the clamping diodes with active switches [29]. The implementation of the active devices, offered more redundancy and options to control the stress distribution, though by the cost of two more devices, gate drivers and also power supplies.

Algorithms that can include multiple control objectives are of special interest for multilevel converter topologies like NPC topologies. Due to the higher number of devices and voltage sources, the complexity of the control algorithm is much higher then for e.g the conventional 2-level VSC's [30]. For example for the 3-level neutral point clamped (NPC) topology in the system configuration shown in the Fig. 1.2, three variables are controlled: the output voltage on the filter capacitor, DC-link voltage balance and the switching frequency (if no modulator is used). The configuration is normally used for stand-alone converter operations like uninterruptible power supplies [31] or AC microgrids [10]. However, as mentioned before, to keep the converter operation in safe conditions, the most stressed device will define the maximum allowed output power. Not only does this determine the output power, it also affects the converter life-time [32]. It is straightforward that the devices working under higher thermal stress are more prone to fail. Therefore, the balanced thermal distribution is not only out of interest for converter performance but also the reliability. FS-MPC algorithm offers the opportunity to unite all of the mentioned objectives for the NPC topology in a single control loop.

The design process of the FS-MPC algorithm can be divided into three stages depicted in the Fig. 1.4. For the NPC converter 27 different switching combinations can be applied to achieve 19 different voltage vectors, 8 redundant vectors are used to control the neutral point of the DC-link capacitors.

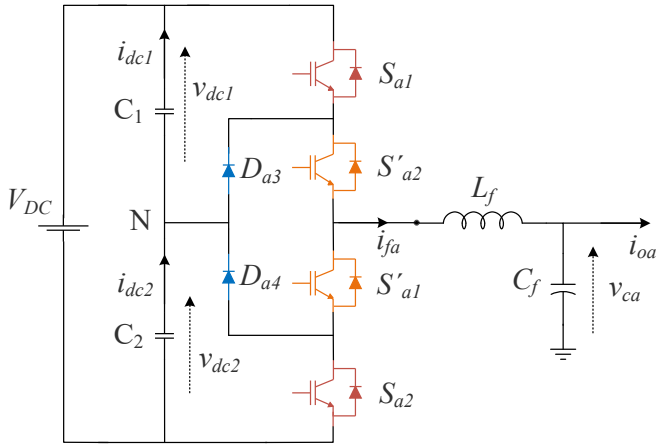

Fig. 1.3: Single phase NPC module scheme with an output LC filter.

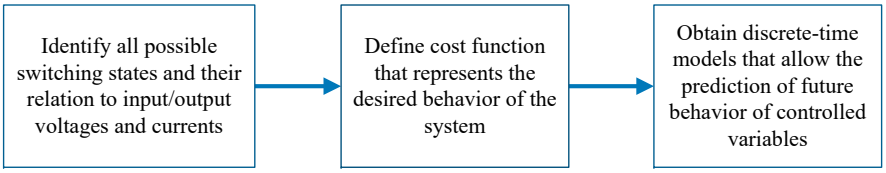

Fig. 1.4: Design flow of the FS-MPC algorithm for power electronic converters.

To control the output voltage of the NPC converter in Fig. 1.2 the cost function needs to contain two objectives: voltage reference tracking and DC-link balancing:

$$g = (v^*_{c\alpha} - v^P_{c\alpha})^2 + (v^*_{c\beta} - v^P_{c\beta})^2 + \lambda_{dc} \cdot g_{dc} \tag{1.1}$$

$$g_{dc} = (v^P_{dc1} - v^P_{dc2})^2 \tag{1.2}$$

where $v^P_{c\,\alpha\beta}$ and $v^P_{dc1,2}$ are the predicted filter and DC-link voltages, $v^*_{c\,\alpha\beta}$ are the defined reference filter voltages and λ_{dc} is the weighting factor. To obtain the predictions of voltages, system equations that define the DC and AC dynamics are used. For predicting the DC dynamics, capacitor voltages $v_{dc1,2}(t)$ and respective charging currents $i_{dc1,2}(t)$ are calculated using the following

equations:

$$v_{dc1,2}(t) = C_{dc1,2}\frac{di_{dc1,2}(t)}{dt} \tag{1.3}$$

$$i_{dc1}(t) = i_{dc}(t) - \sum_{x=a,b,c} H_{1x} \cdot i_{fx}(t) \tag{1.4}$$

$$i_{dc2}(t) = i_{dc}(t) + \sum_{x=a,b,c} H_{2x} \cdot i_{fx}(t) \tag{1.5}$$

H_{1x} and H_{2x} are used as indicator functions. The operation logic is the following: H_{1x} will return 1 if the phase leg $x \in a,b,c$ is connected to $V_{dc}/2$ while H_{2x} returns 1 if the phase leg is connected to $-V_{dc}/2$, otherwise the function returns the value 0. For calculating the future propagation of the capacitor voltage $v_{c\alpha\beta}$, the LC filter equations are used [31]:

$$v_{i\alpha\beta}(t) = L_f\frac{di_{f\alpha\beta}(t)}{dt} + v_{c\alpha\beta}(t) \tag{1.6}$$

$$i_{f\alpha\beta}(t) = C_f\frac{dv_{c\alpha\beta}(t)}{dt} + i_{o\alpha\beta}(t) \tag{1.7}$$

L_f and C_f are filter inductance and capacitance, $i_{f\alpha\beta}$ and $i_{o\alpha\beta}$ are the filter and load currents, $v_{i\alpha\beta}$ are the inverter output voltages. The equations (1.3)-(1.7) are discretized using the forward Euler method as explained in [10]. In each sampling time the discretized equations will be updated with new measurements to calculate the predictions of the voltages for the 27 possible switching combinations. The combinations that will minimize the cost function (1.1) will be applied to the converter switches. In the experimental implementation, the predictions are calculated for two steps ahead to compensate for the computational delay [9].

1.1.2 Applications of neural networks in power electronics

Neural networks (NN) are considered as universal function approximators that can process complex signals in a very short time. They have been implemented in various fields of engineering and they are one of the key elements in development of humanoid robots, photo and video recognition software and autonomous driving systems.

First applications of NN in power electronics originate in the early 90's [33–35]. The main motivation to use NN in power electronics control systems was to reduce the computational burden of the control algorithm. Moreover, the possibility to adapt the NN controller during operation to changing environment conditions was something other control methods could not offer at that time. One of the first applications of the NN controller with experimental implementation was reported in 1994 [36]. Further development of

microprocessor technology opened the door for many more applications in power electronics [37–40].

Using the NN in combination with MPC is a popular solution in control design. NN can be used either for solving the optimization problem of the model predictive controller [32] or to create a system model and afterwards apply the MPC algorithm [41, 42]. In [42] the use of NN in imitation learning settings is presented for quadrotors controller. The Model Predictive Contouring Control (MPCC) is here used as a supervisor to help the controller learn to follow the path and avoidance obstacles. Another example for autonomous aerial vehicle controller is presented in [43]. The MPC algorithm has again taken the role of the supervisor, collecting the observation data under full state observation, which is utilized to train a NN policy. After the training is completed, the NN is able to chose control actions based only on observations from vehicles sensors.

NN can also be used to synthesise controllers e.g. a robust model predictive controller [44], conventional model predictive controller [45] and for finite-set model predictive controller [46]. In this Ph.D. project two applications of neural networks in MPC will be demonstrated: optimization of weighting factors in the cost function and creation of a high accuracy imitator of the FS-MPC power electronics controller.

1.2 Project motivation and research goals

As mentioned in the previous section, the use of model predictive control for controlling the multilevel converters can bring many advantages compared to the traditional linear based control algorithms like [20]:

- applications in multi-variable systems
- fast dynamic response
- non-linearities and constraints can easily be included
- nested control loops are replaced by a single control loop
- simple implementation of the controller

Considering these advantages, the overall research question for this Ph.D. project can be formulated as follows:

- Can the FS-MPC algorihms bring new advantages in terms of control simplicity and performance to multilevel converter applications?

To answer this question, we have to be aware that there are still some limitations that are stopping the full potential of this advanced control method in industrial applications [11, 20–22]:

- missing method for optimum design of the cost function
- missing tools for stability assessment
- missing tools for performance and robustness assessment
- high computational burden of algorithms for multilevel topologies and especially in multi-step prediction horizon applications

Thus the goal of this Ph.D. project is to propose and validate solutions which can remove the mentioned limitations and introduce new tools that can help this control method further development in the power electronics control applications. In order to achieve this goal, advanced methods and tools with origins in the statistics and computer science will be adapted for the power electronics control applications. Moreover, the thermal stress distribution in multilevel converters, which defines the output power, efficiency and in long term the reliability of the converter, needs also to be analysed. Such findings can be used to propose a FS-MPC based algorithm that would provide a more evenly distributed thermal stress among the devices and increase the reliability.

The main objectives of this dissertation can be summed up in the following research questions:

- How to utilize the FS-MPC algorithm to improve the thermal stress distribution in multilevel converters and not negatively affect the primary control objectives?
- How to optimize the cost function design of the FS-MPC algorithm?
- FS-MPC algorithm is missing a tool to assess the performance and robustness of the algorithm. Can this be done by using a statistical model checking approach?
- How to reduce the computational burden of a FS-MPC without sacrificing the performance or using heuristic search algorithms and extrapolations? Can artificial neural networks (ANN) be used to imitate such FS-MPC algorithm?

These questions will be answered in the same order in the dissertation through the upcoming chapters, that are based on the published journal and conference papers. Published papers are provided in the Appendix of the dissertation.

1.3 Project limitations

Several multilevel converter topologies can nowadays be found in industry and even more in academia. Depending on the structure of the topology or application, different control objectives are used on the control algorithms. Therefore, it is necessary to limit the research of this Ph.D. project to one topology that has a wide application area and a mature technology status. Neutral point clamped topology, more precisely the three-level neutral point diode clamped converter (NPC) and active neutral point clamped converter (ANPC) are selected as the potential application and demonstration topologies for this Ph.D. project. A two level voltage source converter topology has also been used in the project to present the application of optimization of the cost-function design and the use of ANN.

The stand-alone converter configuration with LC output filter, which is typically found in uninterruptible power supply (UPS) systems or AC microgrids is used in the experimental validation of the proposed methods while grid-connected modes were not investigated in this PhD project. Nevertheless, some of the proposed methods can also be applied for grid-connected converters while some will require adaptations to the new control objectives.

Simulations for evaluating the junction temperature and stress distributions of the devices in the NPC and ANPC system models are performed in Plecs. The switching and conducting losses, and thermal parameters are modelled using the data-sheets of the devices used in the experimental set-up and provided by the manufacturer for NPC converter SKiiP 28MLI07E3V1 from Semikron [47, 48]. For the ANPC converter, prototype hybrid SiC 3-level modules from Danfoss are used. At the time the measurements were conducted, the dynamic parameters of the module were not yet available, therefore the data used for modelling was obtained from the chip manufacturer with the same static chip parameters for the static behaviour [49, 50].

1.4 Thesis Outline

The Thesis is divided into two parts: **Report** and **Selected publications**. The **Report** consist out of six chapters, which are based on the nine publications included in **Selected publications** part. The content of each chapter and corresponding publications are summarized as follows:

- **Chapter 1 : Introduction**
  State of art in FS-MPC algorithm and applications for multilevel converters are presented. Ph.D. project motivation, research goals and limitations are explained.

- **Chapter 2 : FS-MPC for improved stress distribution in multilevel**

converters
FS-MPC algorithms for redistribution of thermal stress in a 3-level NPC converter and hybrid A-NPC converter are presented. Simulation and experimental results are analysed to check the effects of the stress redistribution objective on the primary reference tracking objective and secondary DC-link balancing objective.
Based on publications : C1 , C2

- **Chapter 3 : Optimization of the cost function design by ANN**
  An artificial neural network approach for selecting the cost function parameters is explained. The approach is demonstrated on three design cases: design for high performance on 2-level VSC for UPS application, design for improved reliability on 3-level NPC converter for UPS application and design for optimal control of induction motor under different operating conditions. The accuracy of the created ANN surrogate is compared to simulation and experimental results for all three design cases.
  Based on publications : J1 , J2, C3

- **Chapter 4 : Performance verification of the FS-MPC algorithms using the SMC approach**
  Modelling of the power electronics system using the stochastic timed automata is explained. Procedure of modelling and using the statistical model checking to verify the performance of FS-MPC algorithm is presented and applied on two power converter topologies: 2-level VSC and 3-level NPC converter.
  Based on publications : J3, J4, C4

- **Chapter 5 : Supervised imitation learning of model predictive control systems**
  A new approach to controller synthesis of FS-MPC algorithms with high computational burden is presented. An artificial neural network is used to imitate the original FS-MPC algorithm. High accuracy of the imitator is observed in the simulations and experiments. It is confirmed that the computational burden of the FS-MPC algorithm is not increasing with the extension of the prediction horizon.
  Based on publications : J5

- **Chapter 6 : Conclusion**
  All contributions of the Ph.D. project are summarized and future research aspects are given.

1.5 List of Publications

The research outcomes during the Ph.D. study have been disseminated in journal papers and conference publications as listed in the following. Parts of these publications are used in the Ph.D. thesis as previously listed.

Publications in Refereed Journals

J1. T. Dragicevic, **M. Novak**, "Weighting Factor Design in Model Predictive Control of Power Electronic Converters: An Artificial Neural Network Approach," *IEEE Trans. Ind. Electron.*, vol. 66, no. 11, pp. 8870–8880, Nov. 2019.

J2. **M. Novak**, H. Xie, T. Dragicevic, F. Wang, J. Rodriguez, and F. Blaabjerg, "Optimal Cost Function Parameter Design in Predictive Torque Control (PTC) Using Artificial Neural Networks (ANN)," *IEEE Trans. Ind. Electron.*, Status: Under Review.

J3. **M. Novak**, U. M. Nyman, T. Dragicevic, and F. Blaabjerg, "Analytical Design and Performance Validation of Finite Set MPC Regulated Power Converters," *IEEE Trans. Ind. Electron.*, vol. 66, no. 3, pp. 2004-2014, March. 2019.

J4. **M. Novak**, U. M. Nyman, T. Dragicevic, and F. Blaabjerg, "Application of Statistical Model Checking Methods to Finite Set Controlled Converters," *IEEE Ind. Electron. Magazine*, vol. 13, no. 3, pp. 6–15, September 2019.

J5. **M. Novak**, T. Dragicevic, "Supervised Imitation Learning of Finite Set Model Predictive Control Systems for Power Electronics," *IEEE Trans. Ind. Electron.*, 2019, Status: Under Review.

- G. Sugumar, R. Selvamuthukumaran, **M. Novak** and T. Dragicevic, "Supervisory Energy-Management Systems for Microgrids: Modeling and Formal Verification," *IEEE Ind. Electron. Magazine*, vol. 13, no. 1, pp. 26-37, March 2019.

Publications in Refereed Conferences

C1. **M. Novak**, T. Dragicevic and F. Blaabjerg, "Finite Set MPC Algorithm for Achieving Thermal Redistribution in a Neutral-Point-Clamped Converter," *Proc. of IECON*, Washington, DC, 2018, pp. 5290–5296.

C2. **M. Novak**, V. Ferreira, M. Andresen, T. Dragicevic, F. Blaabjerg, M. Liserre, "FS-MPC Algorithm for Optimized Operation of a Hybrid Active

Neutral Point Clamped Converter," *Proc. of ECCE 2019*, Baltimore, MD, USA, 2019, pp 1–7.

C3. **M. Novak**, T. Dragicevic, and F. Blaabjerg, "Weighting Factor Design Based on Artificial Neural Network for Finite Set MPC Operated 3L-NPC Converter," *Proc. of. APEC*, Anaheim, CA, USA, 2019, pp. 77–82.

C4. **M. Novak**, U. M. Nyman, T. Dragicevic, and F. Blaabjerg, "Statistical Performance Verification of FCS-MPC Applied to Three Level Neutral Point Clamped Converter," *Proc. of EPE 2018 - ECCE Europe*, Riga, Latvia, 2018, pp. 1–10.

- **M. Novak**, U. M. Nyman, T. Dragicevic and F. Blaabjerg, "Analytical Performance Verification of FCS-MPC Applied to Power Electronic Converters: A Model Checking Approach," *Proc. of COMPEL*, Stanford, CA, US 2017, pp. 1–6.

Chapter 2

FS-MPC for improved stress distribution in multilevel converters

2.1 Background

In the past few years, optimizing the design of power converters to achieve a desired reliability without over-dimensioning the system has drawn a lot of attention in the power electronics community. To keep a minimum margin in the design is not an easy task, especially in applications with different stressing conditions. The neutral point clamped converter topologies are good examples of a power electronics application where not all components are exposed to the same level of the stress. During operation, the output power of a converter is limited by the maximum allowed thermal stress of the most stressed semiconductor devices. Thus, unequal distribution will limit the output power of the converter and the switching frequency.

The solution of this problem can be found either in modification of the hardware or optimization of the control algorithm. An example of hardware a solution is the ANPC topology, which was introduced in 2001 [23] or an asymmetric power rating selection method as proposed in [51]. However, it is well known that different operating points of the NPC converter don't have the same stress distribution. This means, that the design of the NPC converter using the method in [51] will be optimized only for a certain operating point. Even though a new topology was introduced, the solutions based on the optimization of the control algorithm were still pursued for the conventional NPC topology. Compared to the ANPC topology, the conventional NPC

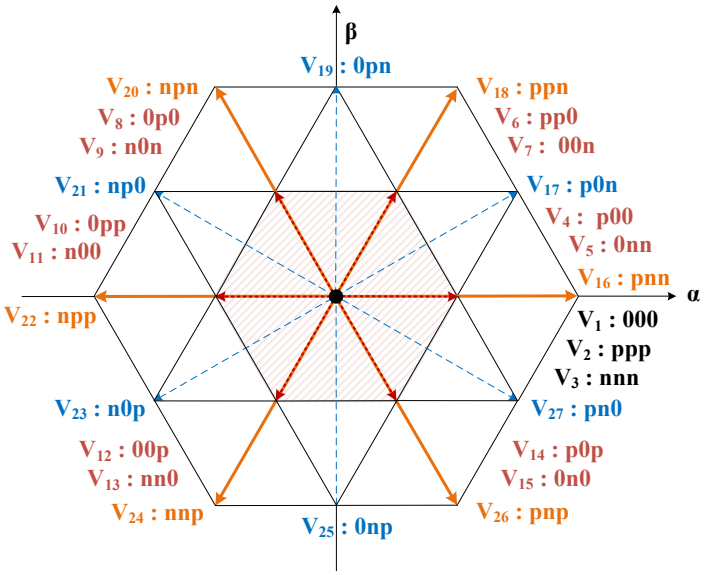

Fig. 2.1: Voltage vectors (28) and switching states that can be generated by a three phase 3L-NPC converter. The notation of the switching states defines the connection of the phase leg output to a positive terminal of the DC-source (p), negative terminal (n) or the neutral point (0). Source:**[C1]**

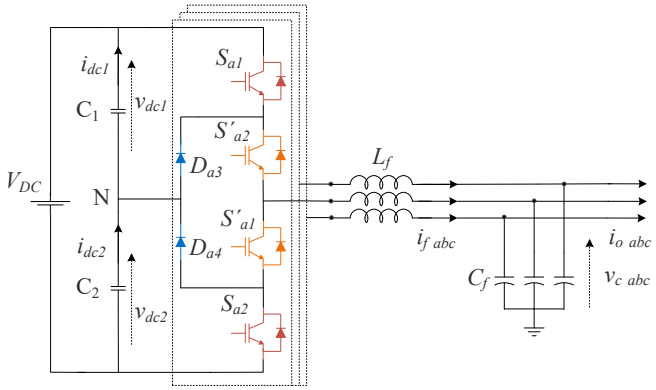

Fig. 2.2: Three phase NPC converter with an output LC filter.

topology has a lower number of components and if a better stress distribution can be achieved only by modifying the control, it would be a less expensive solution.

All solutions based on the control algorithm optimization have one key element in common: the use of the redundant voltage vectors for balancing the thermal stress distribution. In the NPC topology there are 8 redundant vec-

tors as shown in Fig. 2.1. Both conventional linear control methods [28, 52–54] and non-linear methods like predictive control were proposed [8, 19]. In [28] the authors have developed an optimized space vector modulation for low voltage ride through (LVRT) scenarios, where the unequal stress distribution is the most evident and later extended it also to moderate modulation indexes [55]. Other examples of solutions based on the conventional control solution are [52, 53], where the algorithm evaluates a cost function of the device junction temperatures to find the optimal relieving switching sequence. The reason why from the non-linear control methods, MPC was selected to solve the stress distribution problem is an easy inclusion of multiple objectives in the control algorithm. For the NPC topology, following solutions could be applied [8, 19]. In [8] a new expression is added in the cost function for evaluation of the thermal swing based on on-line junction temperature estimations and in [19] the lifetime calculation is included in the cost function. Both of these methods require information about the semiconductor devices and in [19] even information from reliability experiments is required.

In this chapter, a control algorithm based on the FS-MPC for stress redistribution of the semiconductor devices in a NPC topology will be presented. The proposed algorithm:

- does not require any information about the semiconductor devices
- does not require additional measurements like junction temperature measurements
- does not have higher complexity then the conventional FS-MPC

Not only the stress distribution in the NPC converter will be investigated in this chapter, but also in a hybrid SiC ANPC converter. For the ANPC topology, solutions based on PWM stategies [56, 57] and model predictive control [58–60] have been proposed to achieve a balanced stress distribution. In [61] an online calculation of losses is implemented for estimation of the junction temperature of the devices. Afterwards, depending on the current temperature conditions, redundant switching actions are selected from a decision chart. Adaptive double frequency PWM, which uses the duty cycle to optimize the losses is proposed in [57]. It is not shown if for the implementation of this method an outer loop for controlling the DC-link voltage is necessary. The model predictive control algorithms for balancing the device losses were pursued by the research group in [58–60]. The final design in [60], is a combination of space vector modulation (SVM-PWM) and MPC. However, the method was not experimentally validated due to the high computational burden. It was noticed that most of the proposed methods were missing experimental validation and also measurements of the junction temperatures.

For this purpose a prototype converter was build using the 3-level hybrid open modules to measure the device temperatures and analyse the stress distribution in ANPC converter. A comparison of a conventional carrier based control algorithm, proposed for this hybrid configuration in [62], and a model predictive control based control algorithm is performed. The two presented applications are based on publications **[C1]** and **[C2]**.

2.2 FS-MPC algorithm for improved stress distribution in a 3-level NPC converter

The conventional cost function used for voltage control of a 3-level NPC converter shown in Fig. 2.2 has two objectives: minimization of the reference tracking error and balancing of the DC-link capacitor voltages. By using this cost function in the control algorithm we will obtain a junction temperature distribution presented for case $\lambda_t = 0$ in Fig. 2.3 and Fig. 2.4. For all four operating points of the converter a difference in the mean junction temperature of the outer and inner IGBTs can be noticed, and the temperature of the clamping diode is also high. The temperature difference is more pronounced for operating points under nominal current in Fig. 2.3(a) and Fig. 2.4(a).

It is straightforward that if the amplitude of the current flowing through the device is high, so that the device will have to sustain high thermal stress during the switching process. Therefore, if it was possible not to switch the device during this high current periods the stress could be reduced and the junction temperature would drop. In multilevel converter topologies this is possible by using the redundant vectors. Avoiding the switching will of course have a negative consequence on the THD of the converter voltage, thus a balance between these two objectives need to be found.

In the proposed algorithm, to improve the stress distribution from Fig. 2.3 and Fig. 2.4, the added g_t term in the cost function will monitor the amplitude of the current $I_{fx}(k)$ and the switching actions in all three converter phases. It is defined in the cost function as follows:

$$g = (v^*_{c\alpha} - v^P_{c\alpha})^2 + (v^*_{c\beta} - v^P_{c\beta})^2 + \lambda_{dc} g_{dc} + \lambda_t g_t \tag{2.1}$$

$$g_t = |I_{fa}(k)| \cdot n_a + |I_{fb}(k)| \cdot n_b + |I_{fc}(k)| \cdot n_c \tag{2.2}$$

$$n_x = |S_{x1}(k-1) - S_{x1}(k)| + |S'_{x2}(k-1) - S'_{x2}(k)|, \tag{2.3}$$

where $S_{x1}(k)$ and $S'_{x2}(k)$ are the possible switching states of the upper switch (S_1) and inner switch (S'_2), $S'_{x1}(k-1)$ and $S'_{x2}(k-1)$ are the switching states applied in the previous sampling period for converter phases $x \in a, b, c$ and λ_{dc} and λ_t are the weighting factors. The weighting factors can for example be determined using the ANN design approach proposed in Chapter 3. In

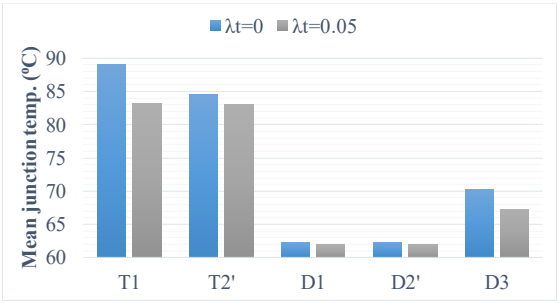

(a) V_{ref} = 400 V I_o = 100 A.

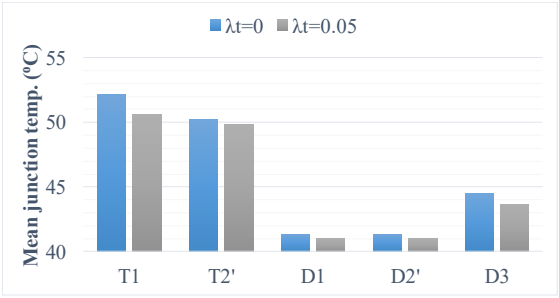

(b) V_{ref} = 400 V I_o = 50 A.

Fig. 2.3: Mean junction temperature comparison for different weighting factors λ_t and converter operating points. Source:**[C1]**

Subsection 3.2.2 an UPS application of the NPC converter with the cost function (2.1) was used to present the design approach for improved reliability of the NPC converter. The ANN was trained using the simulation data. In that case the data-sheet device data is needed to create the thermal model of the devices. For a higher accuracy, experimental measurements should be used to perform the training.

The impact of the cost function (2.1) on the device junction temperatures can be seen for four cases λ_t = 0.05 in Fig. 2.3 and Fig. 2.4. For all operating points of the converter, the junction temperature was reduced and the difference between the outer and inner device temperature was reduced. The temperature drop is also visible for the clamping diode. For the case shown in Fig. 2.4(a) the temperature difference between the inner and outer device was not completely reduced and the inner device was now the one with a higher temperature. This means that the weighting factor for this case needs to be reduced, because the inner switch was switching with a higher frequency than the outer one.

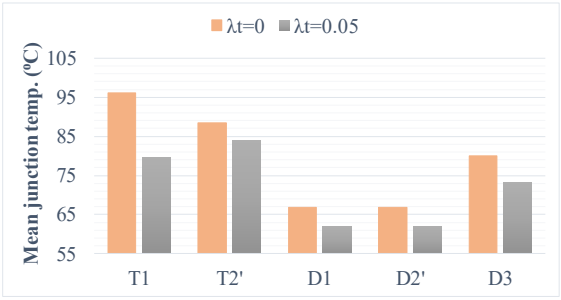

(a) V_{ref} = 280 V I_o = 100 A.

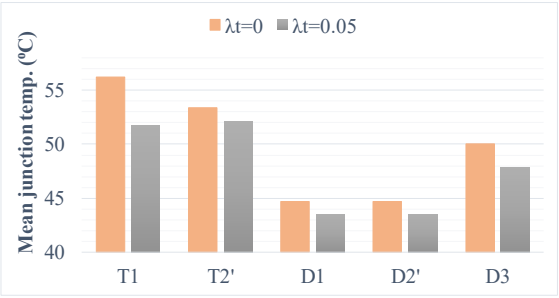

(b) V_{ref} = 280 V I_o = 50 A.

Fig. 2.4: Mean junction temperature comparison for different weighting factors λ_t and converter operating points. Source:**[C1]**

As mentioned before, during the weighting factor tuning it is also necessary to take care of the impact on the output voltage THD and the DC-link

Table 2.1: Evaluated operation conditions of a 3L-NPC converter with and without thermal redistribution. Source:**[C1]**

V_{ref} (V)	I_o (A)	λ_t	THD_{v_c}(%)	$\Delta T_{j1,2'}$ (°C)	T_{jD3} (°C)
400	50	0	0.5	2	44.5
400	50	0.05	0.53	0.8	43.6
400	100	0	0.35	4.5	70.3
400	100	0.05	0.47	0.2	67.3
280	50	0	0.51	3	50
280	50	0.05	0.52	0.3	48
280	100	0	0.35	7.7	80
280	100	0.05	0.53	4	73.3

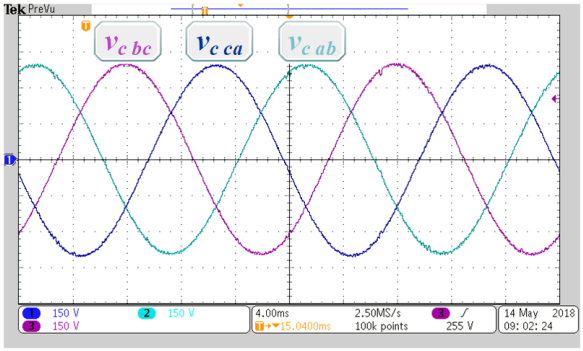

(a) Conventional cost function (λ_{dc}= 1, λ_t=0), THD = 1.29% (150 V/div)

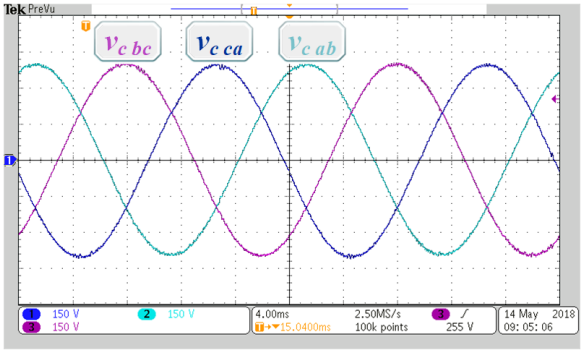

(b) Proposed cost function (λ_{dc}= 1, λ_t=0.9), THD = 1.35% (150 V/div)

Fig. 2.5: Measured output voltage $v_{c\,abc}$ from the 3L-NPC experimental set-up. Source:**[C1]**

balancing performance. In Table 2.1 for the presented four operating points, the impact on the voltage THD can be seen. For the operating points with the high current amplitude the impact is more obvious as the proposed algorithm avoids switching during high current conditions if that is possible. In the experimental set-up the measurements of the output voltage were conducted for the operating point V_c = 230 V and I_o = 8 A to evaluate the impact of g_t on the voltage THD. The parameters of the experimental set-up are given in Table 2.2. For the case without g_t calculated THD was 1.29% with an average switching frequency of 7 kHz and for the case when λ_t = 0.9 the THD was 1.35% with an average switching frequency of 5 kHz. The waveforms can be observed in Fig. 2.5.

Table 2.2: Parameters of the experimental set-up. Source:**[C1]**

Parameter	Value
DC link voltage	V_{DC} = 700 V
DC link capacitors	$C_{dc1,2}$ = 4 mF
Output filter parameters	L_f = 2.4 mH, C_f = 15 μF
Algorithm sampling time	T_s = 25 μs
Weighting factors	λ_{dc} = 1, λ_t = 0.9

2.3 FS-MPC algorithm for improved stress distribution in a 3-level hybrid ANPC converter

In order to satisfy the market's demand for high power density converters with small and light filters, the switching frequency of the converters has to be increased to the level where the thermal stress and switching losses of silicon devices were too high. Thus, wide-bandgap (WBG) devices, which have a superior performance for high switching frequency conditions, were introduced. Not all devices in the converter topology need to be replaced by the WBG devices. By analysing the operating conditions of the converter, only devices producing high switching losses could be replaced by WBG devices, while devices that have longer conducting periods can benefit from Si-IGBT conduction characteristics. In [62–65] examples of hybrid topologies with the proposed modulations are presented.

In this section the temperature and loss distribution will be analysed for a hybrid ANPC converter. The configuration of the 3-level module is shown in Fig. 2.6. The inner devices (S_2, S_3) of the module are SiC MOSFETs, the outer (S_1, S_4) and clamping devices (S_5, S_6) are Si IGBTs. This configuration is preferable for an unidirectional power flow with a high modulation index like photovoltaics, wind turbines or UPS, due to the high stress applied to the inner devices. As mentioned in the introduction, the key to achieve a high power output is to design the control algorithm that would provide a balanced thermal stress distribution. In this application, the control algorithm needs to use the advantage of low switching losses of the SiC MOSFETs.

Eight different switching combinations can be applied to one phase module, two that connect the converter output terminal to the negative DC voltage, two that connect to the positive DC voltage and four that will produce the zero voltage at the output. From the eight possible combinations, four combinations that require only two switches to change the state when transitioning from positive to zero output voltage and negative to zero voltage were selected for application [62, 66]. These switching combinations can be found

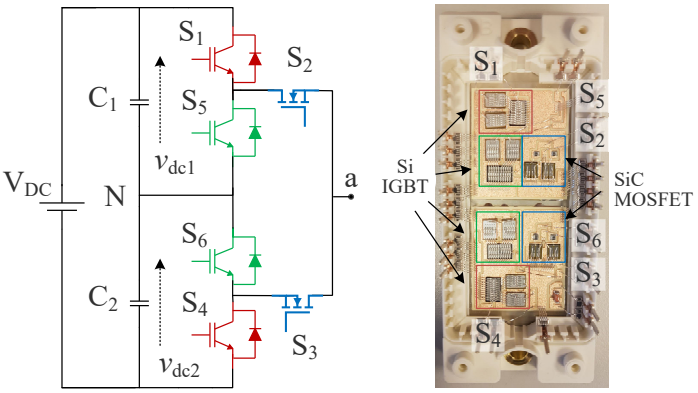

Fig. 2.6: One phase ANPC open module scheme used in the three phase system for validating the control method. Source:**[C2]**

Table 2.3: Switching states of the 3L ANPC converter used in the control algorithm. Source:**[C2]**

Switching state	S_1	S_2	S_3	S_4	S_5	S_6
P	1	1	0	0	0	1
0^+	1	0	1	0	0	1
0^-	0	1	0	1	1	0
N	0	0	1	1	1	0

in Table 2.3. In [62] using these switching combinations, a phase-disposition carried based PWM was applied to the same module configuration as shown in Fig. 2.6. For the applied PWM, only the inner devices are changing the state during each half cycle, while the outer and clamping devices change the state only twice during one period of the modulation signal. However, using this algorithm an outer loop for control of the DC-link voltage is necessary.

Instead of using the phase-disposition carrier based PWM, MPC algorithm can be used to unify the three control objectives (reference tracking, DC-link balancing and stress redistribution) in a single control loop. To efficiently use the inner MOSFET devices, a penalty g_p is introduced to the cost function for switching combinations that require switching of the outer devices:

$$g = (v^*_{c\alpha\,\beta} - v^P_{c\alpha\,\beta})^2 + \lambda_{dc} g_{dc} + \lambda_p g_p \tag{2.4}$$

$$g_{dc} = (v^P_{dc1} - v^P_{dc2})^2 \tag{2.5}$$

$$g_p = \sum_{x=a,b,c} (1 - |S_{2x}(k) - S_{2x}(k-1)|) + (1 - |S_{3x}(k) - S_{3x}(k-1)|), \tag{2.6}$$

where λ_{dc} and λ_p are the weighting factors, $S_x(k-1)$ is the applied switching state in the previous interval and $S_x(k)$ is the current switching state for all converter phase legs $x \in a, b, c$.

Using the simulation model of the ANPC converter system with an LC output filter, device losses and device junction temperatures were compared for the FS-MPC algorithm with a cost function (3.8) and the carrier-based PWM (benchmark algorithm) from [62]. The converter is operated at nominal output power (73 kW) and the switching frequency of the carrier-based PWM controller is set to 15 kHz. For the FS-MPC controller calculated average switching frequency was 14 kHz. Calculation of converter losses showed 1110 W losses (efficiency η = 0.985) for carrier-based PWM controller and 883 W losses (efficiency η = 0.988) for the FS-MPC algorithm. Although, the difference in the efficiency was not significant, the stress distributions were different. Lower losses per device can be spotted for the FS-MPC algorithm in Fig. 2.7(a). The only devices producing the switching losses in the carrier-based PWM algorithm are the MOSFETs. On the other side, the FS-MPC algorithm is not exclusively switching only the MOSFETs. On contrary, switching losses are also spread to the IGBTs, which are not continuously conducting for half of the period like in [62]. Looking at the junction temperatures of the devices in Fig. 2.7(b), a more balanced distribution is also visible.

Due to the limitation of the experimental set-up (PCB design, DC-supply capacity and protection) it was not possible to reproduce the nominal operating conditions used in the simulations. The thermal measurements using an IR camera were performed for load current I_o = 30 A and V_{dc} = 260 V. In Fig. 2.8 the DC-link voltages and the load current waveforms are shown, confirming the good performance of the DC-link balancing control. The average switching frequency of the FS-MPC algorithm was 5.8 kHz, therefore this switching frequency was used to repeat the measurements for the benchmark algorithm. In Fig. 2.9 temperature measurements are shown for the both control methods. For the benchmark model, the measured temperature difference of the outer device and clamping device was 3.8 °C, and for the FS-MPC algorithm it was reduced to half. The difference between the inner and outer device was within 1 °C for both control algorithms.

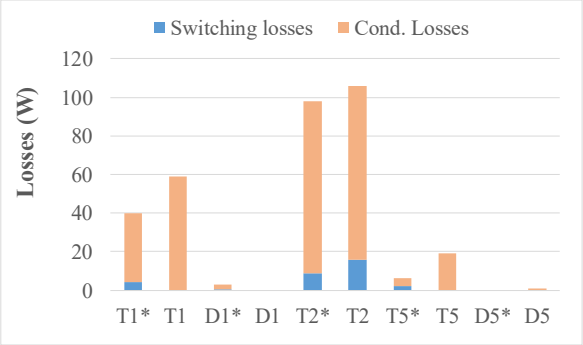

(a) Device losses in a hybrid module for MPC (*) and benchmark algorithm [62].

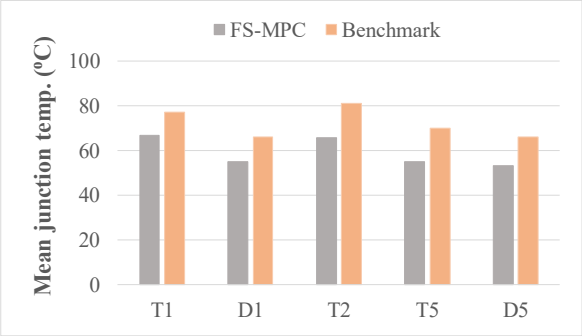

(b) Device junction temperatures in a hybrid module for MPC (*) and benchmark algorithm [62].

Fig. 2.7: Simulation results for 3-level ANPC converter using FS-MPC for stress redistribution. Source:**[C2]**

2.4 Summary

In this chapter it has been demonstrated that FS-MPC algorithm can be used to improve the thermal stress distribution of NPC and ANPC converters. The proposed FS-MPC algorithm for the NPC topology has a simple implementation, no additional measurements are required and the computational efforts are not increased. For converter operation under both high and low amplitude index, it has been shown that the difference between the junction temperatures of the outer and inner devices was reduced and the THD of the output voltage was not significantly increased. Moreover, the stress applied to the clamping diode was also reduced. The most significant drop in the temperature of the devices was observed during the high load current and

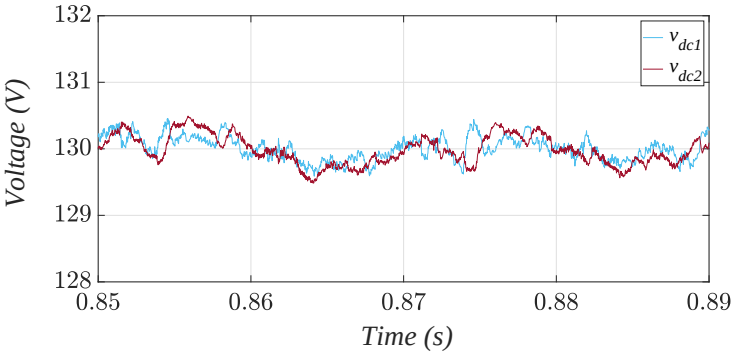

(a) DC-link voltages $v_{dc\,1,2}$

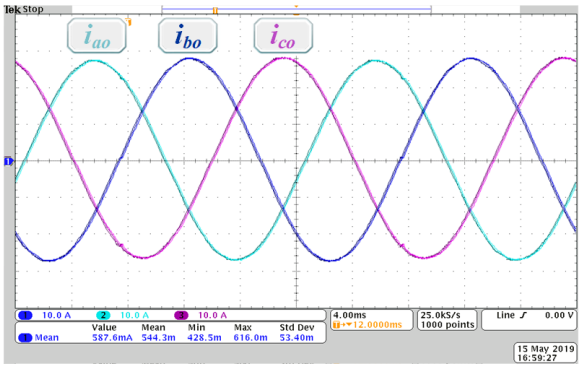

(b) Phase load currents $i_{o\,abc}$ (10 A/div)

Fig. 2.8: Experimental measurements during hybrid ANPC converter operation at P = 4 kW using FS-MPC for stress redistribution. Source:**[C2]**

low reference voltage.

For the presented hybrid configuration of ANPC converter, a simple penalization term in the cost function is sufficient to efficiently utilize the low switching losses of SiC devices. The penalization term ensures that the switching combinations that don't switch the Si devices are preferred. It was experimentally validated that the proposed algorithm can keep the temperature difference between the outer and inner devices at a minimum. Additionally, compared to conventional phase disposition PWM, it can also reduce the temperature difference between the clamping (S_5,S_6) and the outer devices (S_1,S_4).

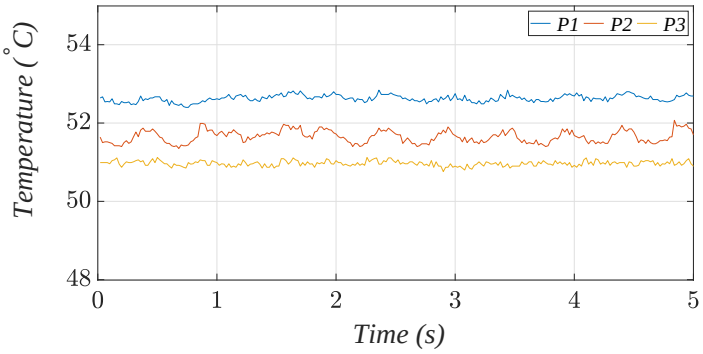

(a) For proposed FS-MPC algorithm.

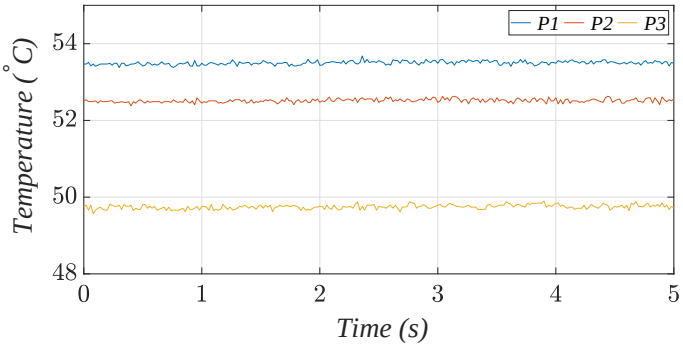

(b) For benchmark algorithm, f_{sw} = 5.8 kHz.

Fig. 2.9: Junction temperature measurement for (P1 → S4 (outer switch), P2 → S3 (inner switch), P3 → S6 (clamping switch) in Fig. 2.6) in steady state, V_{DC} = 260 V, I_o = 30 A. Source:**[C2]**

Based on publications

C1. **M. Novak**, T. Dragicevic and F. Blaabjerg, "Finite Set MPC Algorithm for Achieving Thermal Redistribution in a Neutral-Point-Clamped Converter," *Proc. of IECON*, Washington, DC, 2018, pp. 5290–5296.

C2. **M. Novak**, V. Ferreira, M. Andresen, T. Dragicevic, F. Blaabjerg, M. Liserre, "FS-MPC Algorithm for Optimized Operation of a Hybrid Active Neutral Point Clamped Converter," *Proc. of ECCE 2019*, Baltimore, MD, USA, 2019, pp. 1-7.

Chapter 3

Optimization of the cost function design using ANN

3.1 Background

In the FS-MPC control algorithm, the desired behaviour of the converter system is specified in a multi-objective cost function. The balance of the objectives is defined by the weighting factors. An overview of typically implemented cost functions for applications in power electronics can be found in [20]. It can be observed that in most applications at least one weighting factor is used. The design of these weighting factors is not a simple task, as the complexity of weighting factor design can raise exponentially with every new objective e.g. for a cost function with 3 weighting factors whose range is set from 0 to 10 with a step of 1, this leads to $11^3 = 1331$ possible weighting factor combinations. Therefore, several different approaches for solving the problem of weighting factors design have been proposed.

One of the first methods used for the weighting factor selection was branch and bound search [67]. The positive side of this method is that it is very easy to use but the selection process is still to empirical. An online adaptation of the weighting factors was proposed [68–70], however in the case of [68] it imposed an additional computation burden and in [70] the tuning was performed only with the aim to minimize the objective that has the largest error. Authors of [71] proposed an online tuning based on ANN, where the network is fed by new measurements in each sample time to keep the performance metrics of the converter within same predefined limits for safe operation. Applications of the genetic algorithm were proposed by the authors in [72, 73] where the drawback of the method proposed in [72] is

that each design objective would require a new set of simulations to perform the optimization of the weighting factors. There were also proposals to omit the use of weighting factors in the cost function [17, 74–78]. This is possible if the two objectives can be joined in one reference value like in [74], where the torque reference in a motor drive has been joined in the flux reference or where the two objectives can easily be split into two cost functions like in [75]. It can be noticed that both approaches are motor drives specific and can not be easily adapted to other converter applications and cost functions.

The objective of this Ph.D. project was to find a weight tuning method that would have the following characteristics [**J1**]:

- Applicable to cost functions with multiple conflicting objectives.
- Not imposing additional computational burden.
- Fast and simple tuning process.
- Guaranteed performance according to user-defined design criteria.

3.2 Application of the ANN cost function design approach

The proposed approach is based on the artificial neural networks (ANN). The design process, depicted in the Fig. 3.1, can be separated into three tasks:

- A. Data generation.
- B. ANN training.
- C. Minimization of the fitness function.

In the first step, it is necessary to collect the data sets that will be used to create a surrogate model of the converter system. The data can be extracted either from the simulation model or from experiments, with the first being obviously a much faster approach due to the possibility of parallelizing the process. Which data performance metrics to use to perform the training depends on the converter topology and the application. In Fig. 3.1 for the stand-alone operation of the 2-level VSC, it was sufficient to collect the THD of the filter capacitor voltage and the average switching frequency for N^2 combinations of the two weighting factors. In the second step, those data sets are used to train the ANN. The advantage of using a surrogate model is also a much lower execution time compared to a simulation model.

For cases where the relationship between the inputs (performance metrics) and outputs (weighting factors) is static, a feed-forward type of ANN is suggested for use [79]. For example the structure of the ANN used in **[C1]** is

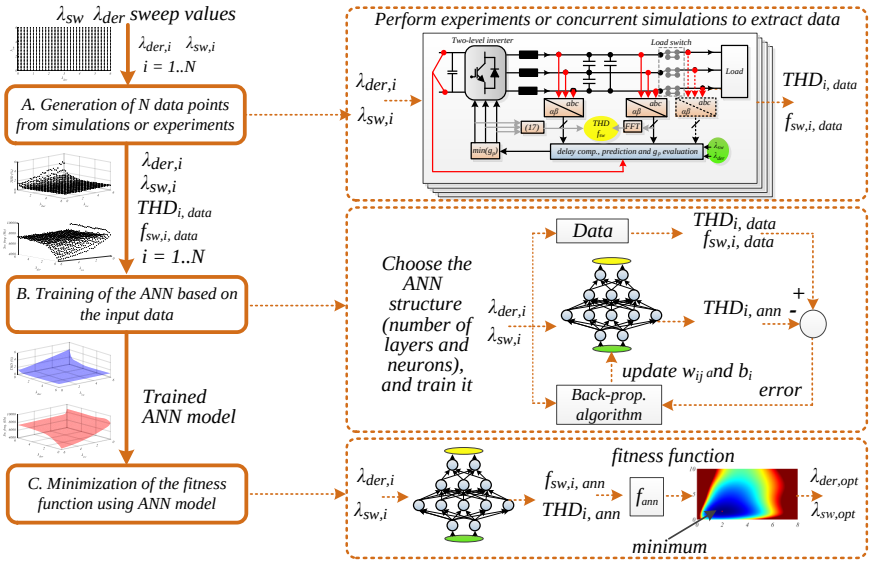

Fig. 3.1: Flowchart of the ANN based weighting factors design in the FS-MPC of power electronic converters. Source: [**J1**]

shown in Fig. 3.2. Three types of layers can be identified: input, hidden and output layers. The output of a each neuron is first multiplied by an associated weight, summed with a bias term and then used to calculate the input of neurons in the next layer. Back-propagation algorithm, which is also implemented in MATLAB's Neural Networks toolbox, is used for training the ANN. In the last step of the design, using the performance metrics, a fitness function f_{ANN} is defined. Minimization of this function will result in an optimized weighting factor combination. In the following subchapters three cost function design applications will be summarized. The applications are based on the publications [**J1**], [**C1**] and [**J2**].

3.2.1 Design for optimum output voltage quality of an UPS system with a 2-level VSC

For this application, the FS-MPC algorithm was implemented with the cost function given in (3.1), which was proposed in [10] for voltage control of an

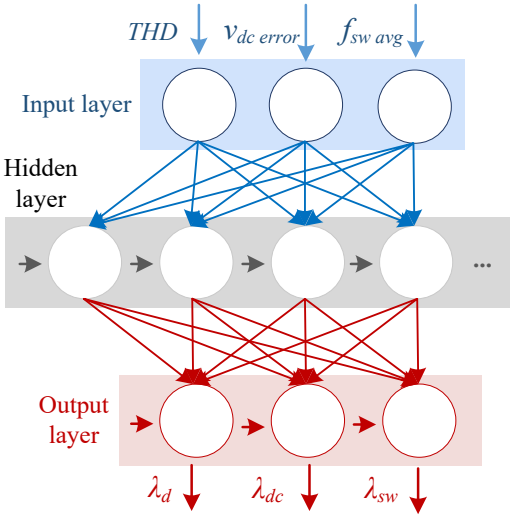

Fig. 3.2: Schematics of a feed-forward artificial neural network (ANN) structure. Source: [**C1**]

AC microgrid or an UPS system presented in Fig. 1.2:

$$g = \left(v_{c\alpha}^{P} - v_{c\alpha}^{*}\right)^2 + \left(v_{c\beta}^{P} - v_{c\beta}^{*}\right)^2 + \lambda_d g_d + h_{lim} + \lambda_{sw} g_{sw}^2 \quad (3.1)$$

$$g_d = (i_{f\alpha}^{P} - i_{o\alpha} + C_f \cdot \omega_{ref} \cdot v_{c\beta}^{*})^2 + (i_{f\beta}^{P} - i_{o\beta} - C_f \cdot \omega_{ref} \cdot v_{c\alpha}^{*})^2 \quad (3.2)$$

$$g_{sw} = \sum_{x=a,b,c} |S_x(k) - S_x(k-1)|. \quad (3.3)$$

where v_c^P and v_c^P* are the predicted voltage value and the reference value of the filter capacitor voltage, i_f^P and i_o are the predicted filter current and measured load current values, ω_{ref} is the reference frequency, C_f and L_f are the output filter parameters, h_{lim} is the current limiting term, $S_x(k)$ is the applied switching state of the converter and $S_x(k-1)$ is the previous one. Two objectives can be identified in the presented cost function with weighting factors (λ_d, λ_{sw}): minimization of the reference tracking error and minimization of the switching frequency.

As mentioned, the first step in the design approach is data collection from the simulation model. For this purpose two performance metrics were defined: THD of the filter capacitor voltage and the average switching frequency $f_{sw\,avg}$. Overall, 441 simulations were performed for different weighting factor combinations. These data sets were used to train the ANN. Using the performance metrics two fitness functions can be structured:

$$f_{ANN,1} = THD_{ANN}^2 \quad (3.4)$$

$$f_{ANN,2} = THD_{ANN}^2 + 3 \cdot f_{ANN\,sw}^2 \quad (3.5)$$

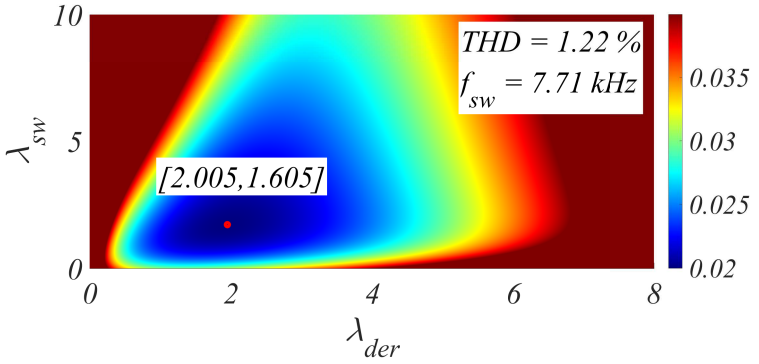

(a) Plot for the fitness function f_{ANN} given in (3.4). Obtained optimum weighting factors: λ_d = 2.005 and λ_{sw} = 1.605.

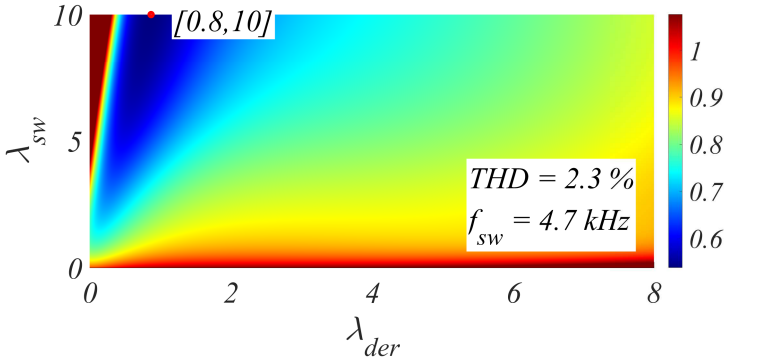

(b) Plot for the fitness function f_{ANN} given in (3.5). Obtained optimum weighting factors: λ_d = 0.8 and λ_{sw} = 10.

Fig. 3.3: Obtained optimal weighting factors for proposed fitness functions. Source:[**J1**]

In (3.5) coefficient 3 was chosen arbitrary to put more importance on the frequency minimization. The two fitness function plots showing the optimal weighting factor combinations are presented in Fig. 3.3. These weighting factors were used in simulation model and the experiments shown in Fig. 3.4 to test the accuracy of the performance metrics predicted by the ANN. A summary of these simulations and experiments is shown in Table 3.1. It can be observed that predicted performance metrics from the ANN match very well the responses of the simulation model (<3% error) and fairly well the metrics obtained in the experimental setup (<10% error).

Extended experimental validations of the obtained cost function parameters for different loads, parameter mismatch and transient response can be found in [**J1**]. Guidelines and results of the weighting factor design for opti-

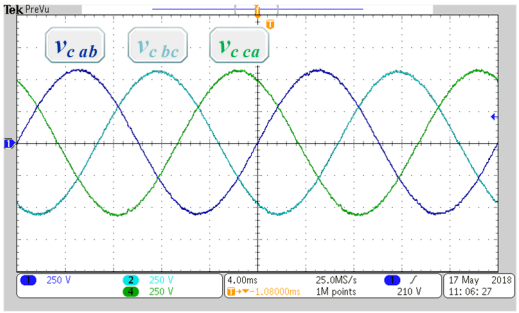

(a) Waveforms for λ_d = 2.005 and λ_{sw} = 1.605 (250 V/-div).

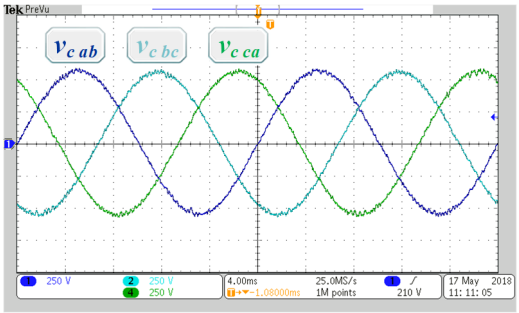

(b) Waveforms for λ_d = 0.8 and λ_{sw} = 10 (250 V/div).

Fig. 3.4: Capacitor voltage measurements from the experimental set-up for R_{load} = 60 Ω and V_{ref} = 325 V. Source:**[J1]**

Table 3.1: Performance metrics results from simulation model, experiments and ANN predictions. Source:**[J1]**

Fitness function	$f_{ANN,1}$		$f_{ANN,2}$	
Perf. metrics	THD	f_{sw}	THD	f_{sw}
Simulations	1.22%	7.64 kHz	2.32%	4.7 kHz
Experiments	1.31%	7.22 kHz	2.31%	5.14 kHz
ANN prediction	1.22%	7.71 kHz	2.3%	4.7 kHz

mum output voltage quality of an UPS system with a 3-level NPC converter can be found in **[C1]**. In the presented case the complexity of the optimization problem was even higher, as three weighting factors were needed to be selected (λ_d, λ_{dc}, λ_{sw}). A good accuracy of the predicted performance metrics by ANN, simulation and experimental results was also observed for this case.

3.2.2 Design for improved reliability of an UPS system with a 3-level NPC converter

In this application the objective of the weighting factor design is to find an optimal trade-off between the THD of the capacitor filter voltage and the thermal stress distribution of the devices in a NPC converter shown in Fig. 2.2. For this purpose the cost function (3.6) proposed in Chapter 2 is used:

$$g = (v^*_{c\alpha} - v^P_{c\alpha})^2 + (v^*_{c\beta} - v^P_{c\beta})^2 + \lambda_{dc} g_{dc} + \lambda_t g_t \tag{3.6}$$

The simulations were performed for λ_{dc} with the range from 0 to 8 and in step of 0.5 and for λ_t with a range from 0 to 0.8 with a step of 0.05 and at the nominal load current i_o = 100 A. In total 17^2 = 289 data sets containing the THD of the capacitor filter voltage THD_v, DC-link capacitor voltage deviation $\Delta v_{dc\,1,2}$ and junction temperature difference of the outer and inner IGBT ΔT_j were collected. The procedure was also repeated for i_o = 10 A, which can be experimentally validated in the 3-level NPC set-up that was at disposal for the project. For this example the fitness function was structured as follows:

$$f_{ANN} \quad = \quad THD^2_{ANN} + \alpha \cdot \Delta T^2_{jANN} + \beta \cdot \Delta v^2_{dc\,1,2\,ANN} \tag{3.7}$$

The coefficients α and β are selected as follows. First α is set to 1, and β is increased step-wise until the effects of the DC-link balancing are visible in the f_{ANN} plot i.e. it should be visible in the plot that if λ_{dc} is close to zero the f_{ANN} value is high (red surface in Fig. 3.5), in this way the condition of taking into account the weighting factor combinations with a good balance is accomplished. In the next step the α value can be tuned. This value is defining the balance between the THD_{ANN} and the $T_{j\,ANN}$. If the value of α is set to 1, then the fitness function will select the combinations of THD and T_j whose sum is the lowest. Now, here the following scenario can occur: a very low THD with a high temperature difference can be selected. However, that is not in the interest of the optimization. The aim is to find a good trade-off. Therefore, coefficient α can be used to reduce the temperature difference to a desired value. For this value the fitness plot will show, which is the lowest possible THD that we can obtain for this T_j. For further analysis on influence of the α coefficient, the parameter can be sweeped for a few values and a Pareto plot can be obtained to show all pairs of the THD and T_j values that minimize the f_{ANN}. In our example, we have set the α = 1 and β = 1.

If the two fitness function plots for i_o = 10 A and i_o = 100 A are compared in Fig. 3.5, it is easy to observe that the range of the weighting factor in the optimal region for the low current is much wider. The area with very low λ_{dc} = 0.5 has a high fitness function value indicating that the dc-link balance is not accomplished. From the obtained plots we can conclude that for high currents the selection of optimum weighting factors has a much higher effect

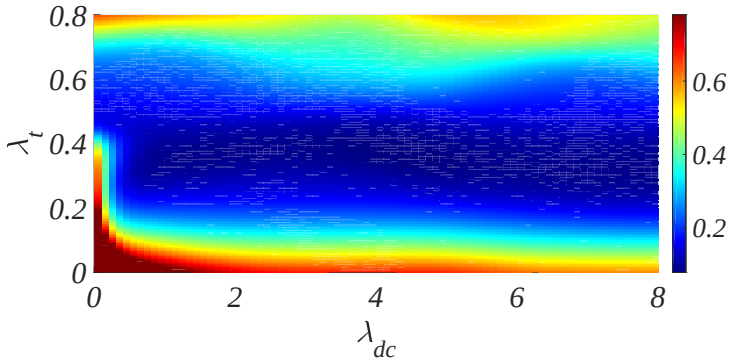

(a) Plot of the fitness function f_{ANN} (3.7) for i_o = 10 A. Obtained optimum weighting factors: λ_{dc} = 6.7 and λ_t = 0.43.

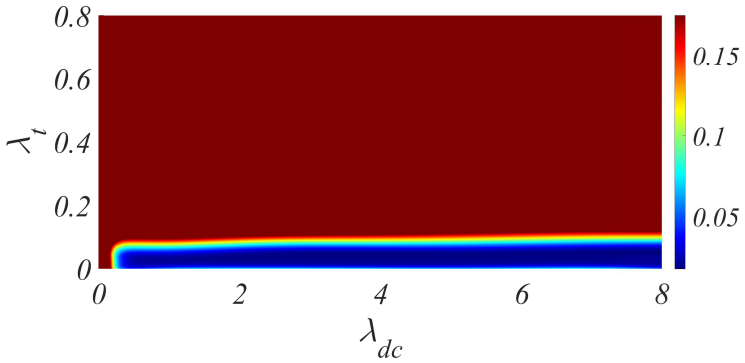

(b) Plot of the fitness function f_{ANN} (3.7) for i_o = 100 A. Obtained optimum weighting factors: λ_{dc} = 7.97 and λ_t = 0.05.

Fig. 3.5: Obtained optimal weighting factors for proposed fitness function of the NPC converter.

on the performance metrics of the converter. On the other hand, higher current will also cause a higher life-time consumption of the converter. Using the weighting factor combinations that minimize the f_{ANN} for different current amplitudes, a cost function with dynamic weighting factors could also be used. A dynamic cost function that takes into account the loading of the converter can be of a great benefit for systems like UPS, where the load is variable. Those combinations can easily be put into a look-up table and selected according to the current amplitude. It must be noted that compared to the online optimization of the weighting factors using the ANN in [71], with this method we can obtain not only the weighting factors adjusted for the safe operation of the converter but also we can guarantee the performance.

In Table 3.2 the performance metrics predicted by ANN and metrics ob-

Table 3.2: Comparison of metrics from ANN, simulation model and experimental set-up (i_o = 10 A, R_{load} = 30 Ω).

Metrics	ANN results	Sim. model results	Experimental results
THD	1.81%	1.89%	2.1%
f_{sw}	5.9 kHz	6 kHz	6.1 kHz
$v_{dc\,error}$	< 1.5 V/period	< 1.5 V/period	< 1.5 V/period

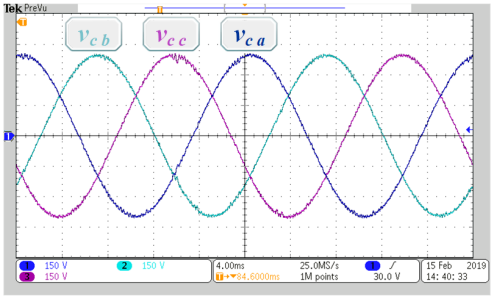

(a) Filter capacitor voltages (150 V/div).

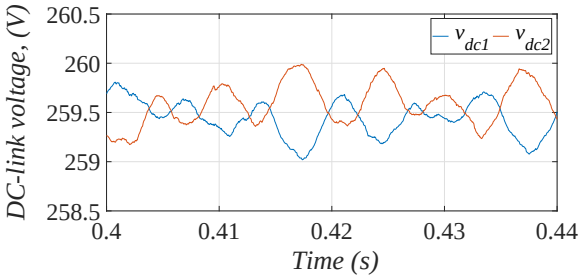

(b) DC-link capacitor voltages

Fig. 3.6: Experimental measurements for i_o = 10 A, R_{load} = 30 Ω and cost function weighting factors: λ_{dc} = 6.7 and λ_t = 0.43.

tained from the simulation model and the experiments are shown in Fig. 3.6 and compared. In the NPC set-up available for this project it was not possible to measure the junction temperature. However, due to the fact that the cost function is affecting the switching frequency, this performance metrics was used for the comparison of the trained ANN prediction accuracy. It can be seen that the error for the ANN predicted THD is below 10% and the f_{sw} is below 5%. It would also be interesting to evaluate the case for NPC converter topology with a life-time consumption being one of the performance metrics.

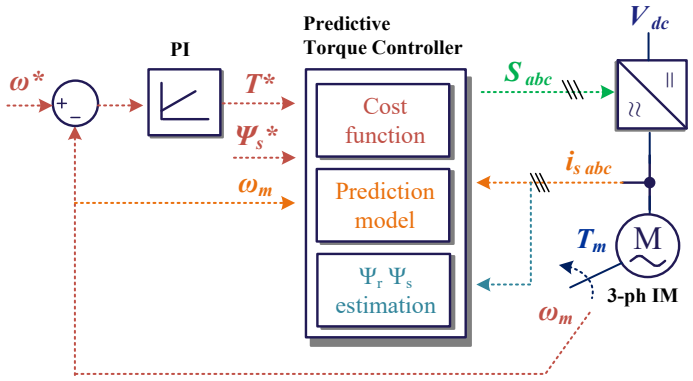

Fig. 3.7: Predictive torque control (PTC) for a three phase VSC drive system. Source: **[J2]**

3.2.3 Design for optimum control of a motor drive

The presented weighting factor design approach can also be used for optimization of the cost function parameters for predictive torque control (PTC). Typical implementation includes a PI speed reference controller, flux estimator and a predictive controller as shown in the scheme in Fig. 3.7. This design optimization has also a complexity N^3 as in the cost function we have two objectives: minimization of the torque error and of the flux error, and we can also add the switching frequency minimization. Therefore, three parameters (λ_Ψ, λ_{sw}, $\Psi_\mathbf{s}$) need to be tuned in the cost function:

$$g = \left| T^* - \hat{T}^{k+2} \right| + \lambda_\Psi \left| \|\Psi_\mathbf{s}^*\| - \|\hat{\Psi}_\mathbf{s}^{k+2}\| \right| + \lambda_{sw'} \cdot g_{sw} + h_{lim} \quad (3.8)$$

$$h_{lim} = \begin{cases} 0, \text{ if } |\bar{i}_s| \leq i_{max} \\ \infty, \text{ if } |\bar{i}_s| > i_{max} \end{cases} \quad (3.9)$$

$$\lambda_{sw'} = \frac{T_{nom}}{\Psi_{nom}} \lambda_{sw} \quad (3.10)$$

where T^*, Ψ_s^* are reference values of the torque and flux and $T_{nom}, \Psi_{s\,nom}$ are the nominal values. h_{lim} is limiting the stator current to the maximum permitted value i_{max}. Before starting the data collection for the ANN training, following performance metrics were defined: mean torque (T_{mean}), torque rms error (T_{error}), RMS stator flux error and current error ($\psi_{s\,error}$, $I_{s\,error}$), time needed to reach 98% of the reference speed at drive start (t_{rise}) and the average switching frequency ($f_{sw\,avg}$)**[J2]**. 512 simulation runs were performed for $\lambda_\Psi = [1.6, 2.8...10]$, $\lambda_{sw} = [0, 0.1, ..., 0.7]$ and $\Psi_s^* = [0.65, 0.7, ...1]$ for T_{load} = 5 Nm. The range for weighting factors was adjusted to sweep only combinations that can lead to a successful motor drive start and operation under loading conditions.

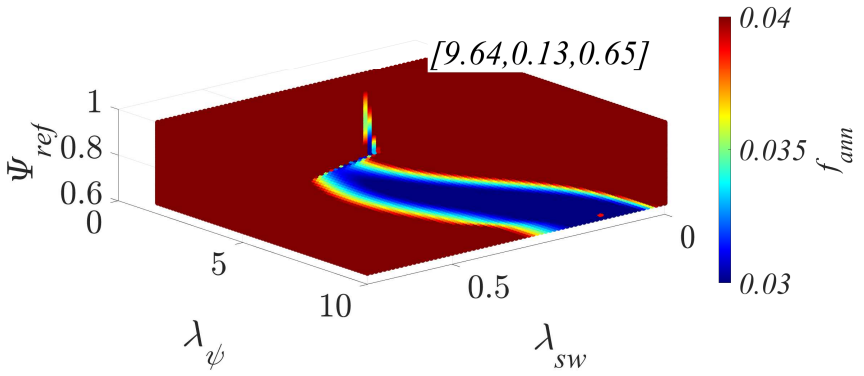

Fig. 3.8: Plot of the fitness function (3.11) for f_1 = 2.5 kHz, ω_{ref} = 200 rad/s, T_{load} = 5 Nm. Obtained optimum parameter values: λ_{ψ} = 9.64; λ_{sw} = 0.13 and ψ^* = 0.65. Source: **[J2]**

Using the performance metrics a fitness function can be defined to find cost function parameters that will guarantee a low stator flux error, stator current error and torque error for example for a average switching frequency of f_1 = 2.5 kHz:

$$f_{ANN} = \psi^2_{s\,error} + I^2_{s\,error} + T^2_{s\,error} + (f_1 - f_{sw\,avg})^2 \tag{3.11}$$

In Fig. 3.8 the plot of the fitness function is presented for T_{load} = 5 Nm and ω_{ref} = 200 rad/s. Plots for T_{load} = 2 Nm and ω_{ref} = 150 rad/s can be found in **[J2.]**. For lower load values, the region of optimal cost function parameters is larger. Both load values cover a wide range of λ_{Ψ} but the range of optimum $\Psi_{\mathbf{s}}$ is very narrow. For a lower reference speed the range of optimum $\Psi_{\mathbf{s}}$ is much wider. If this procedure is repeated, full torque-speed characteristic of the drive can be obtained.

Similar to the previous design cases, the predicted ANN performance metrics were compared to the metrics from the simulation model and the experiments in Table 3.3 and a very good accuracy was observed with the simulation model metrics. A difference between the experiments and the ANN metrics is due to simulation model simplifications. Better accuracy can be obtained by using a detailed simulation model or using the experimental data. A more detailed model will also prolong the duration of the first step in Fig. 3.1. Using the obtained optimum cost function parameter values, experiments were performed for a test profile that includes start of the drive, reversing and loading. The results of the experiments can be observed in Fig. 3.9. Average switching frequency measured in the steady state was 2.3 kHz, which is only 8% lower than the set reference frequency.

Table 3.3: Comparison of performance metrics in steady state operation from ANN and simulation model. Source: **[J2]**

Metrics	ANN	Simulation model (Error)	Experiments
$f_{sw\,avg}$	2.56 kHz	2.54 kHz (20 Hz)	2.32 kHz
$\psi_{s\,error}$	$<$ 0.004 Wb	$<$ 0.004 Wb (0 Wb)	$<$ 0.06 Wb
T_{error}	0.35 Nm	0.32 Nm (-0.03 Nm)	0.5 Nm
$I_{s\,error}$	0.39 A	0.4 A (-0.01 A)	0.37 A

3.3 Summary

In this chapter a new method is proposed for weighting factor design in the FS-MPC applied to power electronics systems. The method is using a surrogate model, which is a result of ANN training on datasets obtained from the simulation models of the systems. The surrogate model can very fast reproduce the optimum weighting factor combination for a user-defined fitness function. A high accuracy was observed with respect to the simulation model (< 5% error) and a very good match with the experimental results (< 10% error) for the presented applications. If desired, the experimentally obtained data sets can be used to achieve an even better accuracy of the performance metrics predicted by the ANN and the experiments. The proposed method is applicable for solving optimization problems of much higher complexity than it was presented for weighting factor design methods based on heuristic methods, genetic algorithms or other ANN based approaches.

Based on publications

J1. T. Dragicevic, **M. Novak**, "Weighting Factor Design in Model Predictive Control of Power Electronic Converters: An Artificial Neural Network Approach," *IEEE Trans. Ind. Electron.*, vol. 66, no. 11, pp. 8870–8880, Nov. 2019.

J2. **M. Novak**, H. Xie, F. Wang, T. Dragicevic, J. Rodriguez, and F. Blaabjerg, "Optimal Cost Function Parameter Design in Predictive Torque Control (PTC) Using Artificial Neural Networks (ANN)," *IEEE Trans. Ind. Electron.*, Status: Under Review.

C3. **M. Novak**, T. Dragicevic, and F. Blaabjerg, "Weighting factor design based on Artificial Neural Network for Finite Set MPC operated 3L-NPC converter," *Proc. of. APEC*, Anaheim, CA, USA, 2019, pp. 77–82.

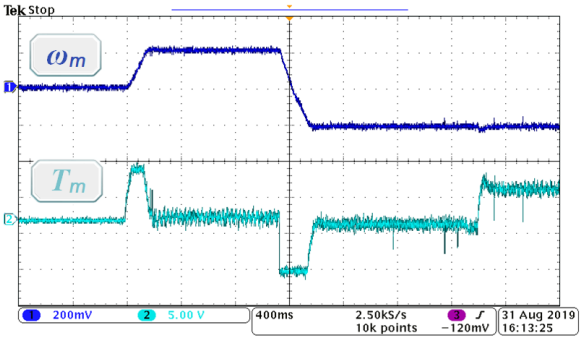

(a) Drive speed (200 rad/s /div) and torque waveforms (5 Nm/div).

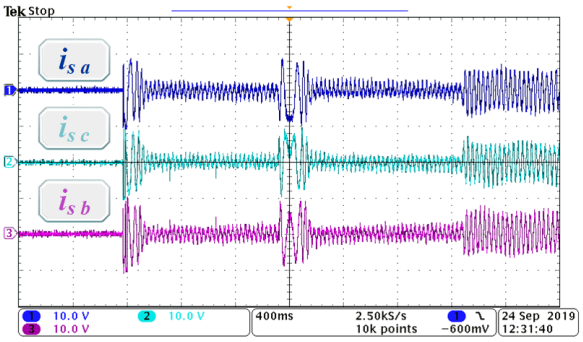

(b) Stator current waveforms (1 Wb/div).

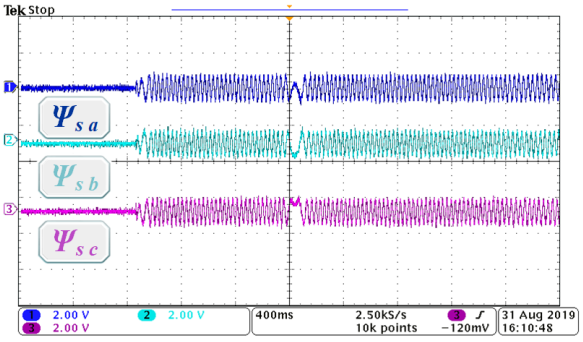

(c) Stator flux waveforms (10 A/div).

Fig. 3.9: Drive start, reversing and loading profile measurements (T_{load} = 5 Nm, f_1 = 2.5 kHz, λ_ψ = 9.64; λ_{sw} = 0.13 and ψ^* = 0.65). Source:**[J2]**

Chapter 4

Performance verification of the FS-MPC algorithms using the SMC approach

4.1 Background

While conventional linear controllers can rely on matured methods and tools for optimization of the design, performance validation and stability verification, for the FS-MPC algorithm the methods and tools to perform the aforementioned tasks still need to be fully developed. In this chapter, a new approach for verifying the performance of the FS-MPC algorithms is presented. The performance verification of a power electronics controller has to verify that the control algorithm can handle the disturbances in the system and at the same time keep minimum deviations of the controlled variables from the set references. As the performance verification method that could be easy applicable to different FS-MPC algorithm applications was not yet established, the performance shown in publications was typically validated by running multiple simulations doing some parameter sweeps or by doing experiments [80–82]. Performing multiple experiments can be rather time consuming compared to running multiple simulations, which can be parallelized using multiple processor cores of the computer. Nevertheless, both approaches lack the reliability of the procedure as there is no guarantee that a finite number of performed experiments can ensure that no errors have been left undetected or even instabilities.

Assessment of the FS-MPC algorithm stability has also been attempted

with most progress shown by the authors in [83, 84] where the Lyapunov stability criteria is used to asses the stability. However, only asymptotic stability is assessed under specific conditions and only for linear systems. Moreover, the method still require further development to be applicable for different converter classes and applications. It needs to be mentioned, that the proposed approach for the performance verification can not be used also to verify the stability of the FS-MPC algorithms. Further development of the proposed approach is needed in order also to incorporate this ability.

4.2 Statistical Model Checking Approach

Model checking methods are formal methods, typically used to analyse software systems in computer science. They are suitable for application on systems that have states and defined transitions between them. Using this method, a guarantee that a system has a certain property can be obtained. A control algorithm can be checked for dead-locks using this method and also that unwanted scenarios are prevented by the algorithm, which is e.g. demonstrated in [85] for the supervisory energy management systems.

However, if the system size is large or/and has stochastic components, this method will suffer from state space explosion i.e. the size of the system state space will grow exponentially. In other words, the time, which is needed to check the system, is exponentially increasing with the size of the system. This will of course impose problems for application on large industrial systems. Therefore, instead of trying to apply an exact analysis method i.e. explore the whole state space of the system, statistical analysis has been proposed. Statistical model checking (SMC) uses Monte Carlo algorithms and it is well suited for modelling deterministic and stochastic components of systems [86–90] and thus suitable for power electronic converter systems, which are a mix of both components e.g. the controller is a deterministic component, while the load is typically a stochastic component.

SMC is able to predict the behaviour of the system using the statistical result, which is a result of performing enough independent simulations of the system. The number of necessary simulations is adjusted according to the predefined confidence of the results. It is straightforward that, the higher confidence level is set, the more samples are needed to a have a valid statistical evidence that the evaluated system has certain properties. Hence, SMC can not provide a 100% guarantee for the system properties. Nevertheless, the fact that the confidence level can be arbitrary set by the user, makes it easy and fast to check new system models by setting the initial confidence level to low values.

Several commercial SMC tools are available for use in academia and industry [91]. A short overview of the available tools is provided in [**J5**]. For

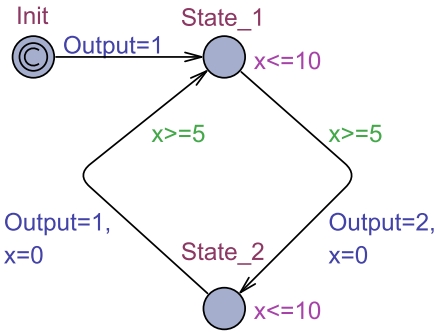

Fig. 4.1: Simple Timed Automaton model in UPPAAL SMC. Source: **[J5]**

the application in this Ph.D. project the UPPAAL SMC toolbox was selected because the modelling language of the toolbox is sufficient for modelling the system presented in this dissertation. A close collaboration with the research group that is standing behind development of this toolbox was also established in order to understand the use of this tool and optimize it for potential future applications.

4.3 Modelling and verification process

UPPAAL tools, used both for model checking and statistical model checking, are based on different versions of Timed Automata (TA) structures. A TA is used to define a timed behaviour and analyse real-time systems. SMC is using networks of Stochastic Timed Automata to model both the stochastic and deterministic system behaviour. In Fig. 4.1 a stochastic TA is presented. Following components of the automaton can be identified: three locations, three transitions and a clock variable x. A clock variable is a special type of variable, whose domain consist of non-negative real numbers. The value of the clock variable is increasing when the automaton is waiting in one location. In this example one time unit of the clock represents 1 μs in the physical world. To each of the locations, the variable Output is assigned. The Init is the initial location of the automaton and it is a committed location, which means that the transition from location Init to State_1 is immediate i.e. no time is passing. The transmission from State_1 to State_2 and vice-versa are guarded by the guards $x >= 5$. The maximum time the automaton can stay in one location is defined by the invariants $x <= 10$.

The exact time of the transitions is not defined, therefore the transitions will happen stochastically in the interval $5 <= x <= 10$. In this example all clock values in the interval $5 <= x <= 10$ have the same probability to trigger the transmission of the automata from from State_1 to State_2 and

vice-versa. By default UPPAAL SMC will set a uniform distribution to all clock x values. Due to this random location changes, in each new simulation a different value of the clock x will trigger the transmissions in the system. This offers many possibilities for modelling stochastic components like converter loads, wind power plants or photovoltaics. For example, a photovoltaic system can be modelled as an automaton with different solar irradiation values. In a similar way, different wind speeds can be used for a wind power plant automaton.

One TA is of course not sufficient to model the whole system, therefore networks of TA are used. The communication between the automata is established through broadcast channels that are used for synchronization of the processes. The concept is the following. If the guard on the transition edge with label *Start!* is satisfied, the transition will emit the broadcast on this channel *Start*. At the same time all the edges that have been labelled by the receiving synchronization label *Start?* will synchronize with the emitting process. For more information on the modelling and UPPAAL SMC the reader is referred to [92].

4.3.1 FS-MPC controlled converter system as a network of timed automata

The first step in the modelling the FS-MPC controlled converter system using the TA is to identify the components of the system, their locations and transitions. In Fig.1.2, which shows the system configuration used for stand-alone application like UPS or AC microgrid, we can identify the following components: voltage source converter, output filter, load, measurement system and control algorithm.

Visualization of a converter with a control algorithm as a TA is straightforward, each switching combination will be one location of the automaton and the transitions are selected by the control algorithm. The control algorithm is a FS-MPC algorithm, which is defined using the discretized system model as explained in Chapter 1. The load model TA will have two locations, high and low load and the transitions will be stochastic as explained for the TA in Fig. 4.1. The measurement system needs to be a simple automata that will forward the measurements to the controller automaton. Using the broadcast channels the operation of the automata will be synchronized with the sampling frequency. Thus, if the components from Fig. 4.2 are transferred to a UPPAAL model, the block scheme presented in Fig. 4.3 can be structured.

In the example TA in Fig. 4.1, the clock variable was used to trigger the transitions of the automata, however the clock variable is not limited only for use as a time representative in the physical world. In UPPAAL SMC toolbox, it is possible to define the clock variables through differential equations. Therefore, using differential equations we can make the system currents and volt-

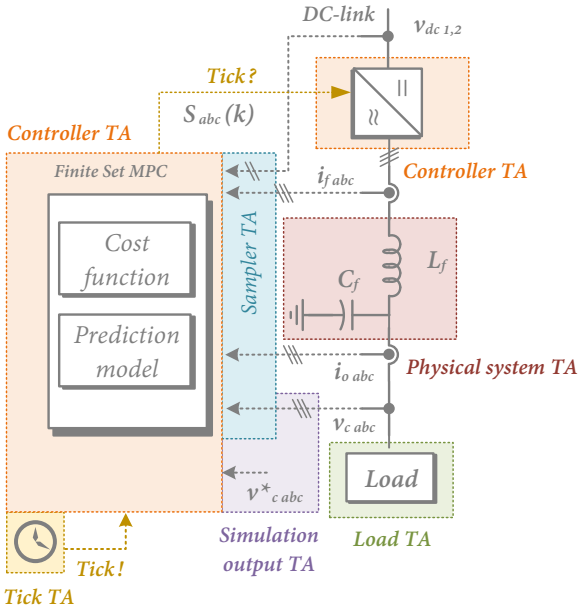

Fig. 4.2: FS-MPC controlled converter system transferred to UPPAAL SMC system model.

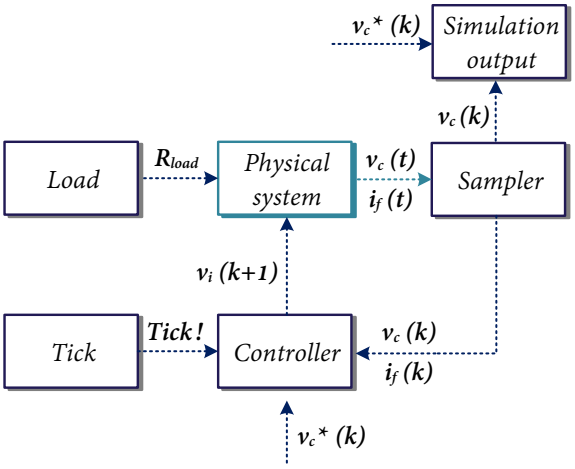

Fig. 4.3: UPPAAL SMC model block scheme of FS-MPC controlled converter system.

ages to take the roles of the global clock variables as shown in the *Physical system* automaton. This means that transitions in the *Controller* automaton, which will represent the converter and the control algorithm in physical

world, will be triggered by the system voltages and currents.

Simplified, in each sample time T_s, the *Sampler* automaton will read the current values of the global clock variables defined in the *Physical system* (v_c, i_f), the *Tick* automaton (used a simple trigger) will broadcast through channel *Tick* to the *Controller* automaton that new measurements are obtained. Using these measurements, the *Controller* automaton will call the FS-MPC algorithm function and calculate the predictions of the system currents and voltages as well as the cost function values for all possible converter switching combinations. After minimization of the cost function values, the inverter output voltage value v_i is updated in the differential equations of the global clocks in the *Physical system*. This value is then used for calculation of the global clock values until the next sampling instance.

The *Simulation output* automaton can be used to calculate certain performance metrics of the system that later can be used for performance validation. In the presented example, the automaton is calculating the difference between the measured capacitor voltage and the reference voltage, and also the rolling average of this value. All automata structures are shown in Fig. 4.4 and Fig. 4.5. More detailed descriptions of single automata components can be found in **[J5]**.

4.3.2 Performance verification

All variables and clocks in the simulation runs can be visualized in Uppaal SMC toolbox, this makes it very easy to compare the waveforms with simulation programs like *Simulink* and check if the modelling procedure was correct. For performance verification the Verifier tool in Uppaal SMC is used. This is done by formulating a query using a defined performance metrics. Three types of questions can be structured in the Verifier and for the application presented in this dissertation the probability estimation question is out of most interest. For the property in question, the Verifier will provide the confidence interval in which the question is true. If the probability question if formulated as follows:

$$Pr[<= 60000]([]diff < 0.05 * 325), \tag{4.1}$$

the Verifier will run multiple time simulations of the model with 60 ms duration of a single simulation and it will monitor if the value of $diff$ is smaller than the set threshold. If the expression is true, it will be encoded as true, if it is not then as false. These results are continuously monitored by a statistical algorithm that resembles Monte Carlo simulation. The user doesn't need to set the number of simulations, the Verifier will determine on its own if enough samples have been provided for statistical evidence that the expression holds. What the user can set before starting the Verifier is the probability uncertainty ϵ.

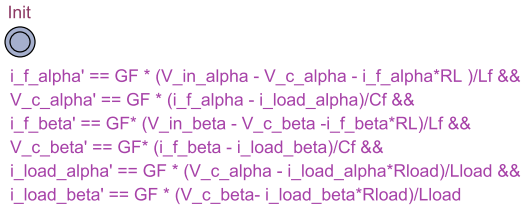

(a) PhysicalSystem.

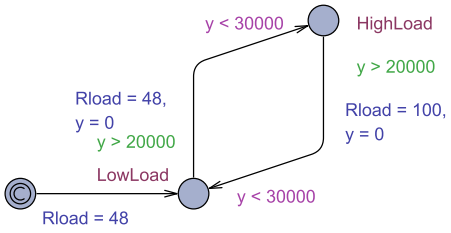

(b) Load.

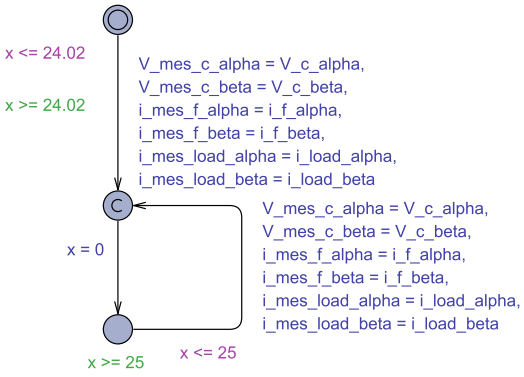

(c) Sampler.

Fig. 4.4: UPPAAL SMC system model components of the FS-MPC controlled converter system. Source:[**J5**]

4.3.3 Application on a 2-level VSC converter

In this subsection the application of SMC approach will be shown on the 2-level VSC converter with a resistive load. The presented results are based on the publication **J4.**. The cost function used in the FS-MPC algorithm is given in (3.1). Before starting the verification, a benchmark Simulink model was created to confirm that the model behaviour in UPPAAL SMC corresponds to the Simulink model. In Fig. 4.6 the capacitor voltage waveforms are presented for the Simulink and the UPPAAL model in the $\alpha\beta$ reference frame

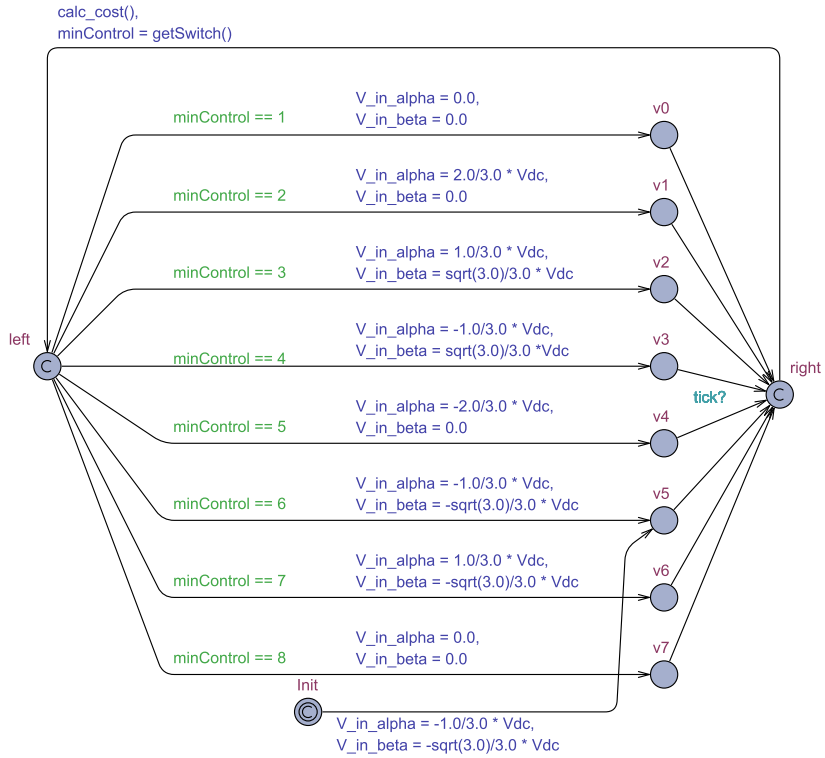

(a) Controller.

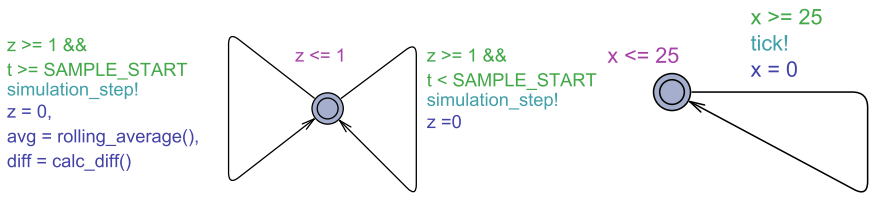

(b) Simulation output. (c) Tick.

Fig. 4.5: UPPAAL SMC system model components of the FS-MPC controlled converter system. Source:**[J5]**

and they both show a good reference tracking performance. The same algorithm was also implemented on an experimental set-up and the measurements have been presented in Fig. 4.6(c). With the performance of both the simulation model and the experiments matching, the model was now ready for the performance verification by using the SMC approach.

Table 4.1: Query probability results obtained from UPPAAL SMC toolbox verifier for a 2-level VSC converter. Source:[**J4**]

Query	Parameter uncertainty	Probability (C1)	Probability (C2)	Probability (C3)
$diff < 8\%$	0	$0.45 - 0.55$	$0 - 0.1$	$0.9 - 1$
$diff < 10\%$	0	$0.89 - 0.99$	$0.19 - 0.29$	$0.9 - 1$
$diff < 12\%$	0	$0.9 - 1$	$0.79 - 0.89$	$0.9 - 1$
$diff < 15\%$	0	$0.9 - 1$	$0.9 - 0.99$	$0.9 - 1$
$diff < 10\%$	-30%	$0 - 0.1$	$0 - 0.1$	$0.78 - 0.88$
$diff < 12\%$	-30%	$0.17 - 0.27$	$0 - 0.1$	$0.9 - 1$
$diff < 15\%$	-30%	$0.81 - 0.91$	$0.47 - 0.57$	$0.9 - 1$
$diff < 10\%$	30%	$0.9 - 1$	$0.8 - 0.9$	$0.9 - 1$

The algorithm's performance was assessed using the following expression:

$$diff \quad = \quad (v^*_{c\alpha} - v^m_{c\alpha})^2 + (v^*_{c\beta} - v^m_{c\beta})^2 \tag{4.2}$$

where $v^*_{c\alpha}$ and $v^*_{c\beta}$ are the real and imaginary parts of reference filter capacitor voltage, $v^m_{c\alpha}$ and $v^m_{c\beta}$ are measurements of the filter capacitor voltage. The resistance in the load automaton is set to change the value stochastically from 48 $\Omega \rightarrow$ 100 Ω. The probability uncertainty ϵ was set to 0.05. As the performance of the FS-MPC algorithm is highly dependent on the quality of the model, parameter variations were also included in the performance verifications. Therefore, queries were tested for 30% overestimation and underestimation of the filter inductance in the system model. Moreover, three weighting factor designs were also compared for these cases:

- Case 1 (C1) - $\lambda_{sw} = 0$, $\lambda_d = 0$
- Case 2 (C2) - $\lambda_{sw} = 0.2$, $\lambda_d = 0$
- Case 3 (C3) - $\lambda_{sw} = 0.5$, $\lambda_d = 0.4$

The obtained results are presented in the Table 4.1. The analysis of the results shows that the weighting factors have a big influence on the reference tracking performance. In the C3 example, the weighting factors were obtained using parameter sweep with the goal to find a combination that would provide a THD of 1.1% and low average switching frequency [**J4**]. For this case even under the parameter uncertainties and load variations the probability of minimal reference tracking error was close to 100%, which is a

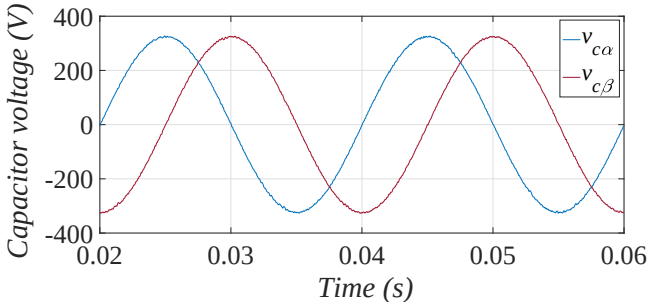

(a) Simulink model.

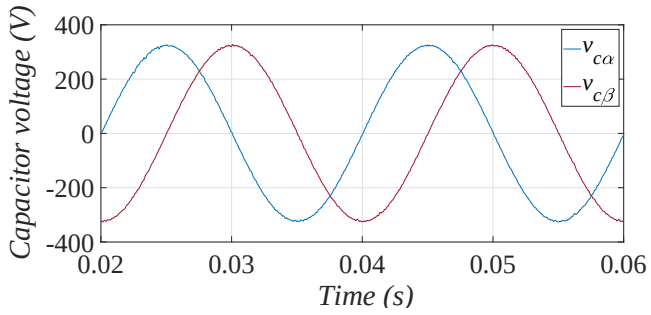

(b) UPPAAL model.

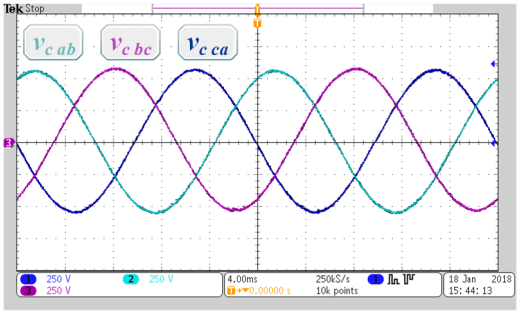

(c) Experiments (250 V/div).

Fig. 4.6: Filter capacitor voltage for 2-level stand-alone VSC system. Source: **[J4]**

very good performance. The C2, as expected due to the priority of switching frequency minimization, showed a significant drop in the reference tracking performance compared to the other two cases. Thus, by properly tuning the weighting factors of the FS-MPC algorithm it is possible to obtain a robust control algorithm that can handle both the parameter uncertainties and load variations. Performance verifications for inductive loads can be found in **[J4]**

4.3.4 Application on a 3-level NPC converter

In this subsection the application of SMC approach will be shown on a 3-level NPC converter with resistive load. The presented results are based on the publication [**C3**]. Following modifications are necessary to convert the 2-level VSC system to a 3-level NPC converter system:

- Define one more global clock in the *Physical system* that will represent one of the DC-link capacitor voltages
- Increase the number of locations in the *Controller* automaton to 27
- In the FS-MPC algorithm add predictions for DC-link voltages and DC-link balancing in the cost function
- Add DC-link voltage measurements to the *Sampler* automaton

It is assumed that the DC-link source provides a constant voltage, thus it was necessary to model the dynamics of only one DC-link capacitor. The cost function used in the FS-MPC algorithm is given in (1.1) and (3.3). The weighting factors λ_d, λ_{dc} and λ_{sw} were selected using parameter sweep in Simulink as shown in [**C3**]. Before using the Verifier tool, the model behaviour in UPPAAL was compared to a Simulink model in the same way as for the 2-level VSC system. In Fig. 4.7 the output filter capacitor waveforms are shown for both models and the experimental set-up. A good performance match is observed in the waveforms, thus it was possible to proceed to the performance verification. The reliability of the probability estimation was set as in the previous case to 95% (ϵ = 0.05). To evaluate the robustness of the algorithm, parameter uncertainties were introduced in the system as 30% overestimated or underestimated values of filter inductance and capacitance.

Obtained results in Table 4.2 show that the probability of the *diff* staying below 6% of the reference value is very high. With the introduced parameter uncertainty, in case of the overestimated filter values (prediction model is using 30% smaller values then defined in the *Physical system*) the probability of the *diff* staying below 6% of the reference value was very low, however the *diff* could still stay below 10% of the reference value with a very high probability. Underestimation of the filter parameters did not degrade the performance of the algorithm. The last column of Table 4.2 also shows the number of runs that were necessary in order to provide the results. Like in previous section, the approach can also be used to verify the performance of different cost functions and weighting factor parameters.

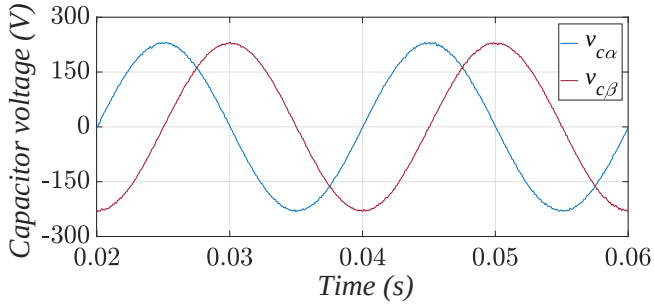

(a) Simulink model.

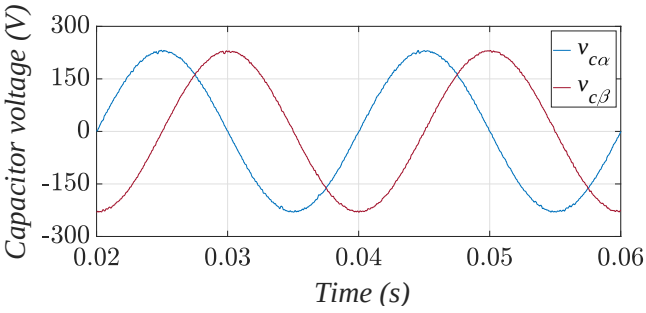

(b) UPPAAL model.

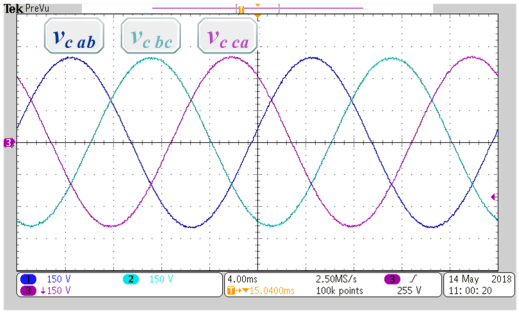

(c) Experiments (150 V/div).

Fig. 4.7: Filter capacitor voltage for 3-level stand-alone NPC converter system. Source: **[C3]**

4.4 Summary

In this chapter it was presented how a statistical model checking approach can be applied for performance verification of a 2-level VSC system and 3-level NPC converter system. The modifications from one converter topology to another can be performed very easily. Comparison of the behaviour of

Table 4.2: Query probability results from UPPAAL SMC toolbox verifier for 3-level stand-alone NPC converter system. Source:**[C3]**

Query	Parameter uncertainty	Probability	No. of sim. runs
$diff < 3\%$	0	0 - 0.097	36
$diff < 6\%$	0	0.874 - 0.974	111
$diff < 3\%$	30%	0 - 0.097	36
$diff < 6\%$	30%	0.901 - 0.999	54
$diff < 6\%$	-30%	0 - 0.097	36
$diff < 8\%$	-30%	0.415 - 0.515	400
$diff < 10\%$	-30%	0.774 - 0.874	238

created models in UPPAAL SMC showed a very good match with the models created in Simulink. Using the approach it is possible to compare the performance of tuned weighting factors in the cost function and also how much the parameter uncertainties in the system model affect the controller performance. It was shown that for very good tuned weighting factors, variations of load and parameter uncertainties will not significantly decrease controller performance.

Based on publications

J4. **M. Novak**, U. M. Nyman, T. Dragicevic, and F. Blaabjerg, "Analytical Design and Performance Validation of Finite Set MPC Regulated Power Converters," *IEEE Trans. Ind. Electron.*, vol. 66, no. 3, pp. 2004-2014, March. 2019.

J5. **M. Novak**, U. M. Nyman, T. Dragicevic, and F. Blaabjerg, "Application of Statistical Model Checking Methods to Finite Set Controlled Converters," *IEEE Ind. Electron. Magazine*, vol. 13, no. 3, pp. 6–15, September 2019.

C3. **M. Novak**, U. M. Nyman, T. Dragicevic, and F. Blaabjerg, "Statistical Performance Verification of FCS-MPC Applied to Three Level Neutral Point Clamped Converter," *Proc. of EPE 2018 - ECCE Europe*, Riga, Latvia, 2018, pp. 1–10.

Chapter 5

Supervised imitation learning of FS-MPC control systems

5.1 Background

In the application of the FS-MPC algorithm for multilevel converters with many different switching states and/or algorithms with longer prediction horizons, the high computational burden presents to be a problem. Many simplifications like heuristic sorting algorithms [93], cost function modifications [94] or the use of extrapolations [16, 95] were proposed to reduce the number of switching combination candidates. However, the proposed solutions sacrifice the control performance in order to reduce the computational burden of the algorithm.

In this chapter a solution based on a computational light signal-processing structure, whose performance is comparable to the original FS-MPC controller, is proposed. So, instead of using a conventional FS-MPC controller, an ANN will be trained off-line to serve as its imitator with one very important benefit: lower computational burden. The execution time of the imitator controller depends on the number of neurons in the network, while the execution of a FS-MPC depends on the prediction horizon length. A fast training data generation process will also be explained. Compared to the NN approach presented in [39], only one hidden layer is needed for controlling all the switched in the converter topology. Moreover, a higher accuracy of the imitator is also observed. The application presented in this chapter is based on publication [**J6**].

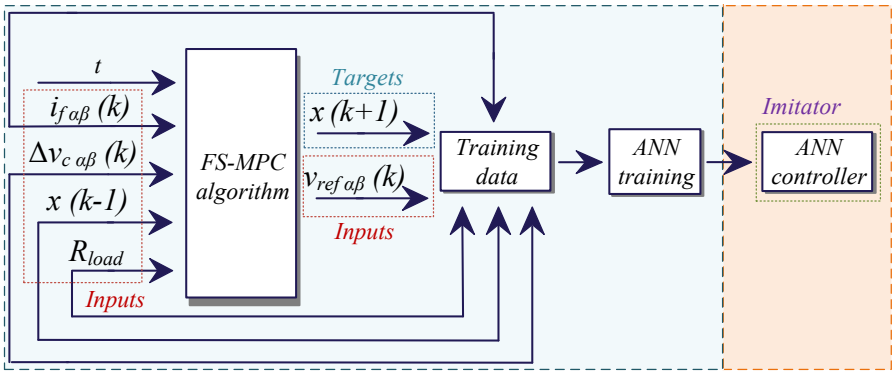

Fig. 5.1: ANN controller synthesis scheme. Source: **[J6]**

5.2 Input data generation

Before the imitator controller can be created, training data needs to be generated. This is a very important process, as the quality of the data will have a big impact on the imitator controller performance. To generate the data, it is not necessary to use a simulation model of the system, using just the FS-MPC algorithm function is sufficient and much faster. Therefore, by using parallel processor cores it is possible to generate 140 million data vectors in less than 3 minutes.

The data generation part is the first stage of the controller synthesis scheme as illustrated in Fig. 5.1. The FS-MPC algorithm accepts seven system variables: time (t), filter currents ($i_{f\alpha\beta}$), deviation of the capacitor voltages ($\Delta v_{c\alpha\beta}$), applied voltage vector from the previous sampling period (x(k-1)) and the load resistance (R_{load}). For these inputs, three output variables are calculated: future optimum switching combination (x(k+1)) and the reference voltage variables ($v_{ref\alpha\beta}$). In the following example, the application given in a 2L-VSC converter for a UPS system configuration with the cost function (3.1) is considered.

For obtaining the imitator of the FS-MPC controller, a pattern recognition method was used. Thus, the ANN output vector $x(k+1)$ is the desired *Target* with the following structure $[x_1, x_2, x_3, x_4, x_5, x_6, x_7]$. If the selected optimum vector by the algorithm is for example V_1, then x_1 will be 1, and the values of x_2 to x_7 will be 0. The structure of the used network is the following: 8 input neurons, 15 hidden neurons and 7 output neurons. To calculate the weights and biases in the ANN, the scaled conjugate gradient back-propagation algorithm proposed in [96] is used. For training of the network, 70% of randomly selected input data is used. The performance of the training is shown in the confusion matrix plot in Fig. 5.2. Each row of

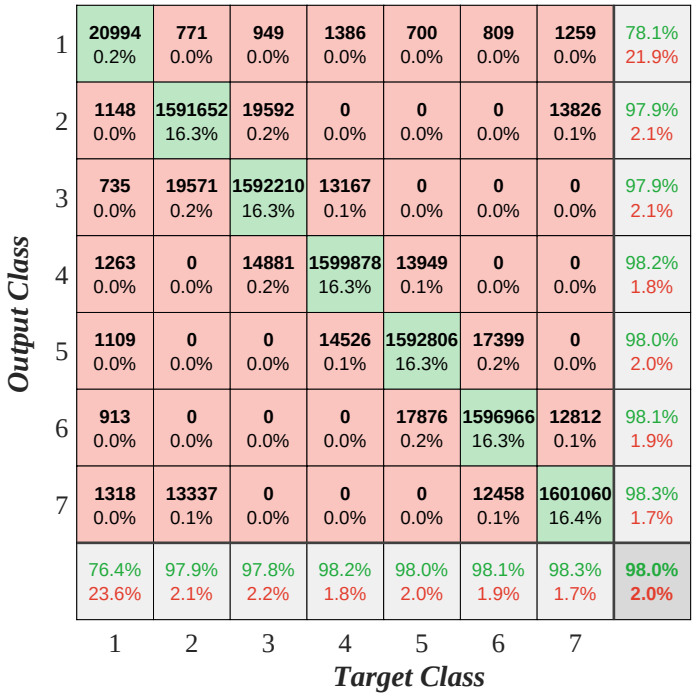

Fig. 5.2: Confusion matrix of the performed ANN training showing the number of correctly (green) and incorrectly(red) classified observations for the FS-MPC imitator controller. Source: [**J6**]

the matrix represents the predicted class and the columns represent the true class i.e. the *Target*. In the diagonal cells it is shown how many observations were correctly classified by the ANN. The performance summary is given in the bottom right cell. For the presented training a very good performance can be observed, with only 2% of incorrectly classified observations. In case this number was much higher (close to 10%) it would be necessary to repeat the training with an ANN structure that has a higher number of neurons in the hidden layer.

5.3 Verification and performance

In the second stage, the trained ANN was exported to Simulink where the performance of the imitator controller on the system presented in Fig. 5.3 was compared to the original FS-MPC controller. Two performance metrics were compared as shown in Table 5.1: THD of the output voltage and the av-

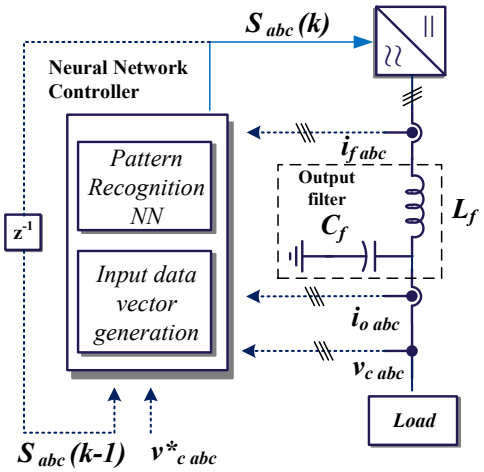

Fig. 5.3: Simplified scheme of the system using the imitator controller. Source: **[J6]**

Table 5.1: Performance metrics results from the simulations and experiments. Source: **[J6]**

	Imitator controller		**Original controller**	
Perf. metrics	THD	f_{sw}	THD	f_{sw}
Simulations	1.42%	8 kHz	1.33%	8.6 kHz
Experiments	1.76%	7.6 kHz	1.69%	8.2 kHz

erage switching frequency. The obtained performance metrics show that the imitator can very well match the performance of the original controller. This was also confirmed in the experimental implementations of the controllers. The THD obtained in the experiments is higher due to the dead time that was not implemented in the simulations. In the experimental set-up load-step change experiments were performed to check if the imitator has also inherited the fast transient response characteristic from the original controller. The measurements presented in Fig. 5.4 have confirmed this. In the introduction it was mentioned that the biggest impact of the proposed controller synthesis would be on multi-step horizon predictions. For this purpose the training of ANN was repeated for a two step prediction horizon and for a three step prediction horizon. The confusion matrix showed that with the same structure of the ANN i.e same number of neurons, the classifications were done with the a constant success rate. Therefore, when the two controllers were implemented in the experimental DSP platform the execution time of a two step horizon and three step horizon imitator was equal to the execution time

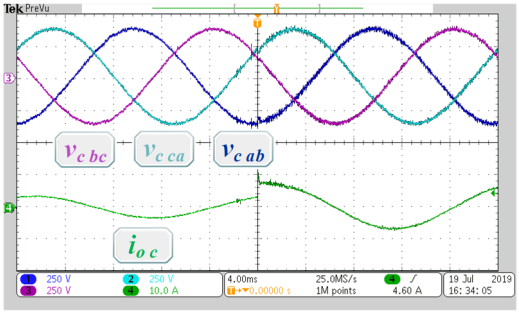

(a) for imitator controller (1-step prediction horizon)

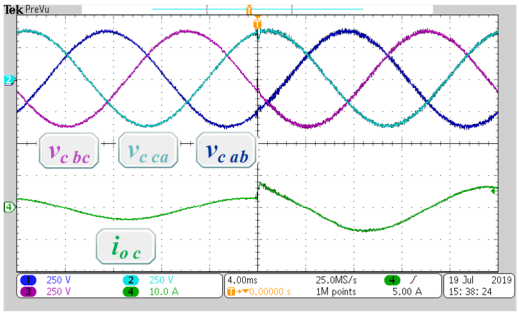

(b) for original FS-MPC controller (1-step prediction horizon)

Fig. 5.4: Filter capacitor voltage (250 V/div) and load current (10 A/div) under load step transient $R_{load} = 60 \rightarrow 30\Omega$. Source: **[J6]**

of the one step horizon imitator. On the other hand, the execution time of the original is increasing exponentially with the horizon length. For the prediction horizon three, the execution without overruns was not possible with the sampling time of 20 μs, which was used in the simulation implementations.

5.3.1 Summary

In this chapter, synthesis of a computationally light power electronics controller, which can imitate the performance of a FS-MPC algorithm, is presented. The proposed approach offers a new opportunity in developing FS-MPC algorithms for applications that are limited by heavy computational burden like multilevel or multi-cell converters and multi-horizon prediction algorithms. It was experimentally validated that the execution time of the imitator controller will not increase if the prediction horizon is extended to 3 steps. Moreover, it was also shown that collecting the data for training a high performance imitator doesn't require a lot of time.

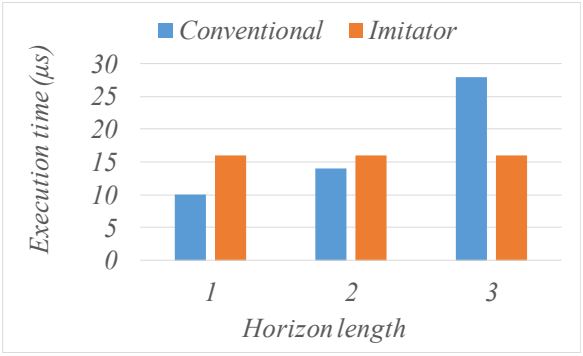

Fig. 5.5: Comparison of the algorithm execution time in DSP and the horizon length. Source: **[J6]**

5.4 Based on publications

J6. **M. Novak**, T. Dragicevic, "Supervised Imitation Learning of Finite Set Model Predictive Control Systems for Power Electronics," *IEEE Trans. Ind. Electron.*, 2019, Status: Under Review.

Chapter 6

Conclusions

6.1 Summary

The aim in this PhD project was to propose solutions to the limitations in the application of FS-MPC algorithm for the multilevel converters and present the advantages this method could bring in to the multilevel converter applications. Some of the proposed solutions are not limited for use only on FS-MPC algorithms. With some modifications they can be used to solve problems in power electronics applications that go beyond the capabilities of the traditional methods.

The biggest advantage of FS-MPC comes from the multi-objective cost function in which it is very straightforward to include new objectives like thermal stress redistribution for the NPC topology. It is well known that unequal stress distribution limits the output power of the converter. The proposed FS-MPC algorithm is trying to mitigate the switching actions in the converter phases during high current periods. This is possible by using the redundant switching states of the multilevel converters. The results have confirmed that if this objective is included in the cost function, the thermal stress distribution is improved and the temperatures of the devices are reduced. Moreover, the effects of the new objective on DC-link voltage balancing and the quality of the output voltage are not overcoming the benefits of the improved stress distribution. It was also shown that it is very simple to adapt the FS-MPC algorithm to hybrid multilevel topologies and obtain the same and in some cases even improved redistribution of the thermal stress compared to conventional carrier based control algorithms. Another advantage of the proposed algorithm is the simple implementation that does not require additional measurements or data-sheet information about the devices and the complexity of the algorithm is not increased either.

The multi-objective cost function needs an approach for tuning the weights of the included objectives. An approach based on artificial neural networks was proposed and validated. The trained ANN acts as a surrogate model of the converter and it is used to rapidly obtain the performance metrics of the system for multiple weighting factor combinations. Using a user-defined fitness function the desired performance of the converter is defined and the minimization of the cost function provides a weighting factor combination with analytical performance guarantee. Very high accuracy of the predictions from ANN with the simulation and experimental results were observed for three different application examples with high complexity optimization problems, which confirms the versatility of the proposed method.

Every control algorithm has to undergo a performance verification before application in the industry and FS-MPC is currently lacking a tool for performing this requirement. Therefore, an approach for performance verification based on Statistical Model Checking was proposed. The proposed approach requires modelling of the power electronics converter system using the stochastic time automata structures. These structures can accurately present both the deterministic components and stochastic components in the power electronics system. To evaluate the FS-MPC algorithm performance in the created model, the user defines a question, which represents the performance criteria. Using the Monte-Carlo algorithms the software will determine the number of simulations it needs to run to provide the probability interval for the defined question. The approach offers the possibility to compare different weighting factor combinations and effects of the parameter uncertainty on the control algorithm performance.

The limitation in the shape of a high computational burden for multilevel converters with many switching combinations or multi-step prediction horizon algorithms could also be removed using the imitation learning. It has been shown that it possible to create an accurate imitator controller of the original FS-MPC controller, whose computational burden will not increase with the extension of the prediction horizon. This opens up many possibilities for implementations of high complexity algorithms.

Overall, it can be noticed that this PhD project united problems, approaches and tools from three different engineering areas: electrical engineering, computer science and mathematics. Moreover, it opened up an interesting collaboration between the power electronics research group and the distributed, embedded and intelligent systems research group. The main objective of this collaboration is to bring a new perspective to control algorithm design for power electronics and develop tools that overcome the limitations of the traditional methods.

6.2 Main Contributions

The main contributions of this PhD project are summarized as follows:

- **FS-MPC algorithm for improved thermal stress distribution in multilevel converters**
  No additional measurements or information about the semiconductor devices are required for the implementation of the proposed algorithm. The complexity of the algorithm is not higher than the complexity of the conventional FS-MPC algorithm. Improvements in the stress distribution are visible in both high and low modulation index operating points. Highest impact of the algorithm is seen under high current and low voltage reference operation.

- **ANN based approach for optimizing the weighting factors in the FS-MPC cost function**
  The proposed approach offers a fast optimization process with analytical guarantee of the desired performance. The approach is applicable to different converter topologies, applications and multi-objective cost functions. With the optimization done offline, no additional computational burden is added to the execution of the FS-MPC algorithm. Predicted performance metrics by the trained ANN have a high correlation with the simulation and the experimental results.

- **Performance validation of FS-MPC algorithm using the statistical model checking approach**
  Using the stochastic timed automata structures it is possible to model both deterministic and stochastic behaviour of a power electronic converter system components. SMC can be used to compare the performance of weighting factors tuning and analyse the effects of the uncertainties in the system on the controller performance. The approach is not exclusive to one topology or application, thus the converter model can easily be adapted to a different converter topology or application.

- **Supervised imitation learning of MPC systems**
  The proposed approach offers an opportunity for implementation of FS-MPC algorithms, without simplifications that sacrifice the performance, for converter topologies that have many possible switching combinations and/or applications that use multi-step horizon predictions. The imitator of the original FS-MPC controller has an ANN structure, which is computationally light and its complexity does not increase for multi-step horizon implementations. Both simulations and experiments confirm the high accuracy and performance of the imitator controller.

6.3 Future Research Perspectives

Presented outcomes of the PhD project have opened up many possibilities for future development of the proposed approaches in power electronics systems:

- The effects of the proposed FS-MPC algorithm for thermal stress redistribution were investigated only for unidirectional power applications. It would be interesting to see if the proposed approach could also be applied for motor drive applications.
- The NPC topology is a popular solution for motor drives applications and especially for industrial applications like rolling-mill machines the stress on the devices is very high. Therefore, it would be of interest to compare the performance of the proposed algorithm on NPC topology and the hybrid ANPC topology solutions. Moreover, impact on the converter life-time should also be investigated and could be included in the cost function.
- The use of dynamic weighting factors for the proposed cost function can also be considered for applications in the further development of the proposed algorithm.
- Statistical model checking approach could be used to compare the performance of different non-linear controllers like ANN controllers in a stochastic environment.
- The UPPAAL software, where the power electronics system was modelled using the stochastic timed automata, was used to validate the performance of the FS-MPC algorithm. By using a software from the same family of tools, there is an opportunity to synthesise a new controller that will also have an analytical guarantee of the stability.
- The application of the supervised imitation learning was presented with an offline ANN training, however an on-line tuning using the new measurements could improve the performance of the control algorithm even more. Moreover, implementation of the imitator on a FPGA platform brings an opportunity to reduce the computation time even more and also expand the time horizon[97, 98].

References

[1] J. I. Leon, S. Kouro, L. G. Franquelo, J. Rodriguez, and B. Wu, "The essential role and the continuous evolution of modulation techniques for voltage-source inverters in the past, present, and future power electronics," *IEEE Trans. Ind. Electron.*, vol. 63, no. 5, pp. 2688–2701, May 2016.

[2] N. Oikonomou, C. Gutscher, P. Karamanakos, F. D. Kieferndorf, and T. Geyer, "Model predictive pulse pattern control for the five-level active neutral-point-clamped inverter," *IEEE Trans. Ind. Appl.*, vol. 49, no. 6, pp. 2583–2592, Nov 2013.

[3] T. Geyer, N. Oikonomou, and G. Papafotiou, "Fast model predictive pulse pattern control," European Patent EP2 891 241B1, Sep. 21, 2016.

[4] P. Cortes, M. P. Kazmierkowski, R. M. Kennel, D. E. Quevedo, and J. Rodriguez, "Predictive control in power electronics and drives," *IEEE Trans. Ind. Electron.*, vol. 55, no. 12, pp. 4312–4324, Dec 2008.

[5] R. P. Aguilera, P. Acuna, P. Lezana, G. Konstantinou, B. Wu, S. Bernet, and V. G. Agelidis, "Selective harmonic elimination model predictive control for multilevel power converters," *IEEE Trans. Power Electron.*, vol. 32, no. 3, pp. 2416–2426, March 2017.

[6] L. Wang, H. Dan, Y. Zhao, Q. Zhu, T. Peng, Y. Sun, and P. Wheeler, "A finite control set model predictive control method for matrix converter with zero common-mode voltage," *IEEE J. Emerg. Sel. Topics Power Electron.*, vol. 6, no. 1, pp. 327–338, March 2018.

[7] R. Vargas, U. Ammann, and J. Rodriguez, "Predictive approach to increase efficiency and reduce switching losses on matrix converters," *IEEE Trans. Power Electron.*, vol. 24, no. 4, pp. 894–902, April 2009.

[8] J. Falck, M. Andresen, and M. Liserre, "Thermal-based finite control set model predictive control for IGBT power electronic converters," in *Proc. IEEE Energy Conversion Congress and Exposition (ECCE)*, pp. 1–7, Sept 2016.

[9] J. Rodriguez and P. Cortes, *Predictive Control of Power Converters and Electrical Drives*, ser. Wiley - IEEE. Wiley, 2012.

[10] T. Dragicevic, "Model predictive control of power converters for robust and fast operation of AC microgrids," *IEEE Trans. Power Electron.*, vol. 33, no. 7, pp. 6304–6317, July 2018.

[11] S. Vazquez, J. I. Leon, L. G. Franquelo, J. Rodriguez, H. A. Young, A. Marquez, and P. Zanchetta, "Model predictive control: A review of its applications in power electronics," *IEEE Ind. Electron. Mag.*, vol. 8, no. 1, pp. 16–31, March 2014.

[12] Y. Xie, R. Ghaemi, J. Sun, and J. S. Freudenberg, "Model predictive control for a full bridge DC/DC converter," *IEEE Trans. on Control Systems Techn.*, vol. 20, no. 1, pp. 164–172, Jan 2012.

[13] S. Sajadian and R. Ahmadi, "Model predictive control of dual-mode operations z-source inverter: Islanded and grid-connected," *IEEE Trans. Power Electron.*, vol. 33, no. 5, pp. 4488–4497, May 2018.

[14] B. Stellato, T. Geyer, and P. J. Goulart, "High-speed finite control set model predictive control for power electronics," *IEEE Trans. Power Electron.*, vol. 32, no. 5, pp. 4007–4020, May 2017.

[15] L. Yan, M. Dou, Z. Hua, H. Zhang, and J. Yang, "Robustness improvement of FCS-MPTC for induction machine drives using disturbance feedforward compensation technique," *IEEE Trans. Power Electron.*, vol. 34, no. 3, pp. 2874–2886, March 2019.

[16] T. Geyer, *Model Predictive Control of High Power Converters and Industrial Drives*. IEEE Wiley, 2016.

[17] F. Donoso, A. Mora, R. Cardenas, A. Angulo, D. Saez, and M. Rivera, "Finite-set model-predictive control strategies for a 3L-NPC inverter operating with fixed switching frequency," *IEEE Trans. Ind. Electron.*, vol. 65, no. 5, pp. 3954–3965, May 2018.

[18] Z. Gong, P. Dai, X. Yuan, X. Wu, and G. Guo, "Design and experimental evaluation of fast model predictive control for modular multilevel converters," *IEEE Trans. Ind. Electron.*, vol. 63, no. 6, pp. 3845–3856, June 2016.

[19] J. Falck, G. Buticchi, and M. Liserre, "Thermal stress based model predictive control of electric drives," *IEEE Trans. Ind. Appl.*, vol. 54, no. 2, pp. 1513–1522, March 2018.

[20] S. Vazquez, J. Rodriguez, M. Rivera, L. G. Franquelo, and M. Norambuena, "Model predictive control for power converters and drives: Advances and trends," *IEEE Trans. Ind. Electron.*, vol. 64, no. 2, pp. 935–947, Feb 2017.

[21] S. Kouro, M. A. Perez, J. Rodriguez, A. M. Llor, and H. A. Young, "Model predictive control: MPC's role in the evolution of power electronics," *IEEE Ind. Electron. Mag.*, vol. 9, no. 4, pp. 8–21, Dec 2015.

[22] V. Yaramasu and B. Wu, *Model Predictive Control of Wind Energy Conversion Systems*, ser. IEEE Press Series on Power Engineering. Wiley, 2016.

[23] A. Nabae, I. Takahashi, and H. Akagi, "A new neutral-point-clamped PWM inverter," *IEEE Trans. Ind. Appl*, vol. IA-17, no. 5, pp. 518–523, Sept 1981.

[24] D. Krug, S. Bernet, S. S. Fazel, K. Jalili, and M. Malinowski, "Comparison of 2.3-kv medium-voltage multilevel converters for industrial medium-voltage drives," *IEEE Trans. Ind. Electron.*, vol. 54, no. 6, pp. 2979–2992, Dec 2007.

[25] H. R. Teymour, D. Sutanto, K. M. Muttaqi, and P. Ciufo, "Solar PV and battery storage integration using a new configuration of a three-level NPC inverter with advanced control strategy," *IEEE Trans. Energy Conversion*, vol. 29, no. 2, pp. 354–365, June 2014.

[26] S. Kouro, J. I. Leon, D. Vinnikov, and L. G. Franquelo, "Grid-connected photovoltaic systems: An overview of recent research and emerging PV converter technology," *IEEE Ind. Electron. Mag.*, vol. 9, no. 1, pp. 47–61, March 2015.

[27] J. Rodriguez, S. Bernet, P. K. Steimer, and I. E. Lizama, "A survey on neutral-point-clamped inverters," *IEEE Trans. Ind. Electron.*, vol. 57, no. 7, pp. 2219–2230, July 2010.

[28] K. Ma and F. Blaabjerg, "Modulation methods for neutral-point-clamped wind power converter achieving loss and thermal redistribution under low-voltage ride-through," *IEEE Trans. Ind. Electron.*, vol. 61, no. 2, pp. 835–845, Feb 2014.

[29] T. Bruckner and S. Bemet, "Loss balancing in three-level voltage source inverters applying active NPC switches," in *Proc. IEEE 32nd Annual Power Electron. Specialists Conf.*, vol. 2, pp. 1135–1140, 2001.

[30] N. Celanovic and D. Borojevic, "A comprehensive study of neutral-point voltage balancing problem in three-level neutral-point-clamped voltage source PWM inverters," in *Proc. Fourteenth Annual Applied Power Electronics Conference and Exposition (APEC)*, vol. 1, pp. 535–541 vol.1, March 1999.

[31] P. Cortes and *et al.*, "Model predictive control of an inverter with output LC filter for UPS applications," *IEEE Trans. Ind. Electron.*, vol. 56, no. 6, pp. 1875–1883, June 2009.

[32] T. Phan, G. J. Riedel, N. Oikonomou, and M. Pacas, "Active thermal protection and lifetime extension in 3L-NPC inverter in the low modulation

range," in *Proc. IEEE Applied Power Electronics Conference and Exposition (APEC)*, pp. 2269–2276, March 2015.

[33] F. Harashima, Y. Demizu, S. Kondo, and H. Hashimoto, "Application of neutral networks to power converter control," in *Conference Record of the IEEE Ind. Appl. Society Annual Meeting,*, pp. 1086–1091 vol.1, Oct 1989.

[34] B. . Lin and R. G. Hoft, "Power electronics inverter control with neural networks," in *Proceedings 8th Annual Applied Power Electron. Conf. and Expo.,*, pp. 128–134, March 1993.

[35] M. R. Buhl and R. D. Lorenz, "Design and implementation of neural networks for digital current regulation of inverter drives," in *Conference Record of the 1991 IEEE Ind. Appl. Society Annual Meeting*, pp. 415–421 vol.1, Sep. 1991.

[36] K. T. Chau and C. C. Chan, "Real-time implementation of an on-line trained neural network controller for power electronics converters," in *Proceedings of 1994 Power Electronics Specialist Conf. - PESC'94*, vol. 1, pp. 321–327 vol.1, June 1994.

[37] X. Fu, S. Li, M. Fairbank, D. C. Wunsch, and E. Alonso, "Training recurrent neural networks with the levenberg marquardt algorithm for optimal control of a grid-connected converter," *IEEE Trans. Neural Networks and Learning Systems*, vol. 26, no. 9, pp. 1900–1912, Sep. 2015.

[38] Y. Sun, S. Li, B. Lin, X. Fu, M. Ramezani, and I. Jaithwa, "Artificial neural network for control and grid integration of residential solar photovoltaic systems," *IEEE Trans. Sustainable Energy*, vol. 8, no. 4, pp. 1484–1495, Oct 2017.

[39] D. Wang, X. Yin, S. Tang, C. Zhang, Z. J. Shen, J. Wang, and Z. Shuai, "A deep neural network based predictive control strategy for high frequency multilevel converters," in *2018 IEEE Energy Conversion Congress and Expo. (ECCE)*, pp. 2988–2992, Sep. 2018.

[40] B. Karanayil and M. F. Rahman, "Artificial neural network applications in power electronics and electric drives," in *Power Electronics Handbook (Fourth Edition)*, fourth edition ed., M. H. Rashid, Ed. Butterworth-Heinemann, 2018, pp. 1245 – 1260.

[41] S. Piche, B. Sayyar-Rodsari, D. Johnson, and M. Gerules, "Nonlinear model predictive control using neural networks," *IEEE Control Systems Magazine*, vol. 20, no. 3, pp. 53–62, June 2000.

[42] S. Stevsic, T. Nageli, J. Alonso-Mora, and O. Hilliges, "Sample efficient learning of path following and obstacle avoidance behavior for quadrotors," *IEEE Robotics and Automation Letters*, vol. 3, no. 4, pp. 3852–3859, Oct 2018.

[43] T. Zhang, G. Kahn, S. Levine, and P. Abbeel, "Learning deep control policies for autonomous aerial vehicles with MPC-guided policy search," in *2016 IEEE International Conference on Robotics and Automation (ICRA)*, pp. 528–535, May 2016.

[44] M. Hertneck, J. Köhler, S. Trimpe, and F. Allgöwer, "Learning an approximate model predictive controller with guarantees," *IEEE Control Systems Letters*, vol. 2, no. 3, pp. 543–548, July 2018.

[45] D. Georges, "A simple machine learning technique for model predictive control," in *2019 27th Mediterranean Conference on Control and Automation (MED)*, pp. 69–74, July 2019.

[46] I. S. Mohamed, S. Rovetta, T. D. Do, T. Dragicevic, and A. A. Z. Diab, "A neural-network-based model predictive control of three-phase inverter with an output LC filter," *IEEE Access*, vol. 7, pp. 124 737–124 749, 2019.

[47] *3-Level NPC IGBT-Module: SKiiP 28MLI07E3V1 datasheet*, Semikron, 6 2016, rev. 1.0.

[48] *3L SKiiP28MLI07E3V1 Evaluation Inverter Technical Explanation*, Semikron, 2014, rev. 2.0.

[49] *PCFG75T65LQW - IGBT datasheet*, ON Semiconductor, 2017, rev. 2.0.

[50] *SCT3022AL - SiC MOSFET datasheet*, ROHM Semiconductor, 2018, rev. 5.0.

[51] U. M. Choi and F. Blaabjerg, "Asymmetric power device rating selection for even temperature distribution in NPC inverter," in *Proc. IEEE Energy Conversion Congress and Exposition (ECCE)*, pp. 4196–4201, Oct 2017.

[52] M. Aly, G. M. Dousoky, E. M. Ahmed, and M. Shoyama, "A unified SVM algorithm for lifetime prolongation of thermally-overheated power devices in multi-level inverters," in *Proc. IEEE Energy Conversion Congress and Exposition (ECCE)*, pp. 1–6, Sept 2016.

[53] M. Aly, E. M. Ahmed, and M. Shoyama, "Thermal stresses relief carrier-based PWM strategy for single-phase multilevel inverters," *IEEE Trans. Power Electron.*, vol. 32, no. 12, pp. 9376–9388, Dec 2017.

[54] T. Bruckner, S. Bernet, and H. Guldner, "The active NPC converter and its loss-balancing control," *IEEE Trans. Ind. Electron.*, vol. 52, no. 3, pp. 855–868, June 2005.

[55] K. Ma and F. Blaabjerg, "Modulation methods for three-level neutral-point-clamped inverter achieving stress redistribution under moderate modulation index," *IEEE Trans. Power Electron.*, vol. 31, no. 1, pp. 5–10, Jan 2016.

[56] G. Zhang, Y. Yang, F. Iannuzzo, K. Li, F. Blaabjerg, and H. Xu, "Loss distribution analysis of three-level active neutral-point-clamped (3L-ANPC) converter with different PWM strategies," in *Proc. IEEE 2nd Annual Southern Power Electronics Conference (SPEC)*, pp. 1–6, Dec 2016.

[57] Y. Deng, J. Li, K. H. Shin, T. Viitanen, M. Saeedifard, and R. G. Harley, "Improved modulation scheme for loss balancing of three-level active NPC converters," *IEEE Trans. on Power Electron.*, vol. 32, no. 4, pp. 2521–2532, April 2017.

[58] D. Andler, M. Perez, J. Rodríguez, and S. Bernée, "Predictive control of three-level active NPC converter with evenly energy losses distribution," in *Proc. International Power Electronics Conference (ECCE ASIA)*, pp. 754–759, June 2010.

[59] D. Andler, J. Weber, S. Bernet, and J. Rodríguez, "Improved model predictive control with loss energy awareness of a 3L-ANPC voltage source converter," in *Proc. International Conference on Applied Electronics*, pp. 1–6, Sept 2010.

[60] D. Andler, E. Hauk, R. Álvarez, J. Weber, S. Bernet, and J. Rodríguez, "New junction temperature balancing method for a three level active NPC converter," in *Proc. European Conference on Power Electronics and Applications (EPE)*, pp. 1–9, Aug 2011.

[61] T. Bruckner and D. G. Holmes, "Optimal pulse-width modulation for three-level inverters," *IEEE Trans. Power Electron.*, vol. 20, no. 1, pp. 82–89, Jan 2005.

[62] Q. Guan, C. Li, Y. Zhang, S. Wang, D. D. Xu, W. Li, and H. Ma, "An extremely high efficient three-level active neutral-point-clamped converter comprising SiC and Si hybrid power stages," *IEEE Trans. Power Electron.*, vol. 33, no. 10, pp. 8341–8352, Oct 2018.

[63] D. Zhang, J. He, and D. Pan, "A megawatt-scale medium-voltage high efficiency high power density "SiC+Si" hybrid three-level ANPC inverter for aircraft hybrid-electric propulsion systems," in *Proc. IEEE Energy Conversion Congress and Exposition (ECCE)*, pp. 806–813, Sept 2018.

[64] J. He, D. Zhang, and D. Pan, "An improved PWM strategy for "SiC+Si" three-level active neutral point clamped converter in high-power high-frequency applications," in *Proc. IEEE Energy Conversion Congress and Exposition (ECCE)*, pp. 5235–5241, Sept 2018.

[65] D. Barater, C. Concari, G. Buticchi, E. Gurpinar, D. De, and A. Castellazzi, "Performance evaluation of a three-level ANPC photovoltaic grid-connected inverter with 650-V SiC devices and optimized PWM," *IEEE Trans. Ind. Appl.*, vol. 52, no. 3, pp. 2475–2485, May 2016.

[66] M. Novak, V. Šunde, N. Čobanov, and Z. Jakopović, "Semiconductor loss distribution evaluation for three level ANPC converter using different modulation strategies," in *Proc. 19th International Conference on Electrical Drives and Power Electronics (EDPE)*, pp. 170–177, Oct 2017.

[67] P. Cortes, S. Kouro, B. L. Rocca, R. Vargas, J. Rodriguez, J. I. Leon, S. Vazquez, and L. G. Franquelo, "Guidelines for weighting factors design in model predictive control of power converters and drives," in *Proc. of IEEE International Conference on Industrial Technology*, pp. 1–7, Feb 2009.

[68] S. A. Davari, D. A. Khaburi, and R. Kennel, "An improved FCS-MPC algorithm for an induction motor with an imposed optimized weighting factor," *IEEE Trans. Power Electron.*, vol. 27, no. 3, pp. 1540–1551, March 2012.

[69] Z. Zhang, W. Tian, W. Xiong, and R. Kennel, "Predictive torque control of induction machines fed by 3L-NPC converters with online weighting factor adjustment using fuzzy logic," in *Proc. IEEE Transportation Electrification Conf. and Expo (ITEC)*, pp. 84–89, June 2017.

[70] L. M. A. Caseiro, A. M. S. Mendes, and S. M. A. Cruz, "Dynamically weighted optimal switching vector model predictive control of power converters," *IEEE Trans. Ind. Electron.*, vol. 66, no. 2, pp. 1235–1245, Feb 2019.

[71] O. Machado, P. Martin, F. J. Rodriguez, and E. J. Bueno, "A neural network-based dynamic cost function for the implementation of a predictive current controller," *IEEE Trans. Ind. Informat.*, vol. 13, no. 6, pp. 2946–2955, Dec 2017.

[72] P. Zanchetta, "Heuristic multi-objective optimization for cost function weights selection in finite states model predictive control," in *Proc. Workshop on Predictive Control of Electrical Drives and Power Electronics PRECEDE*, pp. 70–75, Oct 2011.

[73] P. R. U. Guazzelli, W. C. de Andrade Pereira, C. M. R. de Oliveira, A. G. de Castro, and M. L. de Aguiar, "Weighting factors optimization of predictive torque control of induction motor by multiobjective genetic algorithm," *IEEE Trans. Power Electron.*, vol. 34, no. 7, pp. 6628–6638, July 2019.

[74] Y. Zhang and H. Yang, "Two-vector-based model predictive torque control without weighting factors for induction motor drives," *IEEE Trans. Power Electron.*, vol. 31, no. 2, pp. 1381–1390, Feb 2016.

[75] M. Norambuena, J. Rodriguez, Z. Zhang, F. Wang, C. Garcia, and R. Kennel, "A very simple strategy for high-quality performance of AC machines using model predictive control," *IEEE Tran. Power Electron.*, vol. 34, no. 1, pp. 794–800, Jan 2019.

[76] E. Fuentes, C. A. Silva, and R. M. Kennel, "MPC implementation of a quasi-time-optimal speed control for a PMSM drive, with inner modulated-FS-MPC torque control," *IEEE Trans. Ind. Electron.*, vol. 63, no. 6, pp. 3897–3905, June 2016.

[77] W. Xu, J. Zou, Y. Liu, and J. Zhu, "Weighting factorless model predictive thrust control for linear induction machine," *IEEE Trans. Power Electron.*, vol. 34, no. 10, pp. 9916–9928, Oct 2019.

[78] Y. Yang, H. Wen, M. Fan, M. Xie, and R. Chen, "Fast finite-switching-state model predictive control method without weighting factors for t-type three-level three-phase inverters," *IEEE Trans. Ind. Informatics*, vol. 15, no. 3, pp. 1298–1310, March 2019.

[79] K. Hornik, M. Stinchcombe, and H. White, "Multilayer feedforward networks are universal approximators," *Neural Networks*, vol. 2, no. 5, pp. 359 – 366, 1989.

[80] J. Rodriguez, J. Pontt, C. A. Silva, P. Correa, P. Lezana, P. Cortes, and U. Ammann, "Predictive current control of a voltage source inverter," *IEEE Trans. Ind. Electron.*, vol. 54, no. 1, pp. 495–503, Feb 2007.

[81] R. N. Fard, H. Nademi, and L. Norum, "Analysis of a modular multilevel inverter under the predicted current control based on finite-control-set strategy," in *Proc. Int. Conf. Elect. Power Energy Convers. Syst*, pp. 1–6, Oct 2013.

[82] H. A. Young, M. A. Perez, J. Rodriguez, and H. Abu-Rub, "Assessing finite-control-set model predictive control: A comparison with a linear current controller in two-level voltage source inverters," *IEEE Ind. Electron. Mag.*, vol. 8, no. 1, pp. 44–52, March 2014.

[83] R. P. Aguilera and D. E. Quevedo, "On stability of finite control set MPC strategy for multicell converters," in *Proc. IEEE Int. Conf. Ind. Technol.*, pp. 1277–1282, March 2010.

[84] R. P. Aguilera and D. E. Quevedo, "On stability and performance of finite control set MPC for power converters," in *Proc. Workshop on Predictive Control of Electrical Drives and Power Electronics PRECEDE*, pp. 55–62, Oct 2011.

[85] G. Sugumar, R. Selvamuthukumaran, M. Novak, and T. Dragicevic, "Supervisory energy-management systems for microgrids: Modeling and formal verification," *IEEE Ind. Electron. Magazine*, vol. 13, no. 1, pp. 26–37, March 2019.

[86] A. David, K. G. Larsen, A. Legay, and M. Mikučionis, "Schedulability of herschel revisited using statistical model checking," *Int. J. Softw. Tools Technol. Transf.*, vol. 17, no. 2, pp. 187–199, Apr. 2015.

[87] K. G. Larsen, M. Mikučionis, M. Muñiz, J. Srba, and J. H. Taankvist, *Online and Compositional Learning of Controllers with Application to Floor Heating*. Springer Berlin Heidelberg, 2016, pp. 244–259.

[88] A. Boudjadar, A. David, J. Kim, K. Larsen, M. Mikučionis, U. Nyman, and A. Skou, "Statistical and exact schedulability analysis of hierarchical scheduling systems," *Science of Computer Programming*, vol. 127, pp. 103–130, 5 2016.

[89] T. Mancini, F. Mari, I. Melatti, I. Salvo, E. Tronci, J. K. Gruber, B. Hayes, M. Prodanovic, and L. Elmegaard, "Parallel statistical model checking for safety verification in smart grids," in *Proc. IEEE International Conference on Communications, Control, and Computing Technologies for Smart Grids (SmartGridComm)*, pp. 1–6, Oct 2018.

[90] J. Strnadel, "Predictability analysis of interruptible systems by statistical model checking," *IEEE Design Test*, vol. 35, no. 2, pp. 57–63, April 2018.

[91] M. E. Bakir, M. Gheorghe, S. Konur, and M. Stannett, "Comparative analysis of statistical model checking tools," in *Membrane Computing - 17th International Conference, CMC 2016, Milan, Italy, July 25-29, 2016, Revised Selected Papers*, pp. 119–135, 2016.

[92] K. G. Larsen and A. Legay, *On the Power of Statistical Model Checking*. Springer International Publishing, 2016, pp. 843–862.

[93] B. Gutierrez and S. Kwak, "Model predictive control method with preselected control options for reduced computational complexity in modular multilevel converters (MMCs)," in *Proc. 20th European Conf. on Power Electron. and Appl. (EPE'18 ECCE Europe)*, pp. P.1–P.8, Sep. 2018.

[94] A. Dekka, B. Wu, V. Yaramasu, and N. R. Zargari, "Dual-stage model predictive control with improved harmonic performance for modular multilevel converter," *IEEE Trans. Ind. Electron.*, vol. 63, no. 10, pp. 6010–6019, Oct 2016.

[95] E. Liegmann, P. Karamanakos, T. Geyer, T. Mouton, and R. Kennel, "Long-horizon direct model predictive control with active balancing of the neutral point potential," in *Proc. IEEE International Symp. on Predictive Control of Electrical Drives and Power Electronics (PRECEDE)*, pp. 89–94, Sep. 2017.

[96] M. F. Moller, "A scaled conjugate gradient algorithm for fast supervised learning," *Neural Networks*, vol. 6, no. 4, pp. 525 – 533, 1993.

[97] S. Lucia, D. Navarro, O. Lucia, P. Zometa, and R. Findeisen, "Optimized FPGA implementation of model predictive control for embedded systems using high-level synthesis tool," *IEEE Trans. Ind. Inform.*, vol. 14, no. 1, pp. 137–145, Jan 2018.

[98] P. Falkowski and A. Sikorski, "Finite control set model predictive control for grid-connected AC–DC converters with LCL filter," *IEEE Trans. Ind. Electron.*, vol. 65, no. 4, pp. 2844–2852, April 2018.

ISSN (online): 2446-1636
ISBN (online): 978-87-7210-535-2

AALBORG UNIVERSITY PRESS